

45 **Abstract**

46
47 Creative cognition relies on the ability to form remote associations between concepts, which allows to
48 generate novel ideas or solve new problems. Such an ability is related to the organization of semantic
49 memory; yet whether real-life creative behavior relies on semantic memory organization and its neural
50 substrates remains unclear. Therefore, this study explored associations between brain functional
51 connectivity patterns, network properties of individual semantic memory, and real-life creativity. We
52 acquired multi-echo functional MRI data while participants underwent a semantic relatedness judgment
53 task. These ratings were used to estimate their individual semantic memory networks, whose properties
54 significantly predicted their real-life creativity. Using a connectome-based predictive modeling
55 approach, we identified patterns of task-based functional connectivity that predicted creativity-related
56 semantic memory network properties. Furthermore, these properties mediated the relationship between
57 functional connectivity and real-life creativity. These results provide new insights into how brain
58 connectivity supports the associative mechanisms of creativity.

59

60

61 Teaser: New insight into the neurocognitive determinants of human creativity

62

63

64 Keywords: creativity, semantic network, brain networks, functional connectivity, cognition

65

66

67

68

69

70 Introduction

71 Creativity is key to our ability to cope with change, innovate, and find new solutions to address
72 societal challenges (1). Understanding the complex and multidimensional construct of creativity is thus
73 fundamental to support societal, cultural, and economic progress. Creative behaviors in real life depend
74 on individual differences in cognitive ability, in addition to personality and environmental factors (2).
75 The cognitive mechanisms underlying creative abilities are not yet understood (3–6). The associative
76 theory hypothesizes that creative abilities are related to the organization of semantic associations in
77 memory (7). In support of this theory, several studies found that more creative individuals are able to
78 link distant concepts more easily (8–10), have less common or constrained word associations, and a
79 more flexible organization of semantic memory (9, 11–15). In addition, in brain-damaged patients, rigid
80 semantic associations were associated with poor creative abilities (16–18). Associative thinking has been
81 related to creative abilities as measured within several existing frameworks, such as divergent thinking
82 (8, 9, 14, 19–21), insight problem solving (7, 22), analogical reasoning (23, 24), as well as to creative
83 achievements in real life (25–28). Overall, the properties of semantic memory play an essential role in
84 the cognitive processes that bring forth original ideas.

85 Recent research has demonstrated how computational network science methodologies (29–32)
86 based on mathematical graph theory allow exploring the properties and organization of the concepts in
87 semantic memory via semantic networks (SemNets). Applying these methods, several studies have
88 shown that creative abilities can be related to semantic memory organization (11, 33–38). Kenett and
89 colleagues (11) investigated the SemNets of groups of low and high creative individuals, based on free
90 associations generated by both groups to a list of 96 cue words. They found that the SemNets of low
91 creative individuals were less connected and more spread out compared to the SemNets of high creative
92 individuals. However, estimating SemNets at the group level may obscure individual differences related
93 to creativity. To address this issue, Benedek and colleagues (36) developed a method to estimate
94 individual SemNets, based on word relatedness judgment ratings. Participants rated the relationships
95 between all possible pairs of 28 cue words, serving as a proxy for the organization of these words in an
96 individuals' semantic memory. They demonstrated how individual-based SemNet metrics replicated the
97 group-based findings of Kenett et al. (11), and were related to individual differences in divergent
98 thinking scores (the most widely assessed component of creative thinking) (39, 40). A recent study
99 reported similar results (41). In a previous study, (37) we replicated and extended this finding with two
100 improvements: We controlled the selection of the cue words using a computational method optimizing
101 the distribution of theoretical distances between words, and we assessed creative abilities and behaviors
102 using a more diverse set of tools. This study showed that the network metrics of the individual SemNets
103 correlated with several measures of creativity, including a questionnaire of creative activities and
104 achievements (42). Hence, individual SemNets measures—reflecting the properties of semantic
105 memory—allow exploring underlying cognitive mechanisms of creativity, suggesting that more creative
106 individuals have more flexible semantic associations and connect more distant concepts or words (38).
107 However, the neurocognitive determinants of individual differences in creativity related to the flexibility
108 of semantic associations are still unclear and unexplored.

109 Existing MRI-based neuroimaging studies have identified a large set of brain regions involved
110 in creative cognition (5, 12, 43–47). A growing body of creativity neuroscience research has highlighted
111 the importance of functional interactions within and between several brain networks, including the
112 executive control network, salience network and the default mode network (5, 48). Additionally,
113 semantic and episodic memory regions (44, 49–52) and the motor and premotor regions have been
114 shown to play a role in creative cognition (44, 53). The advantage of a whole-brain functional
115 connectivity approach is to provide a holistic and functional view of how brain networks relate to
116 creative thinking. For example, resting-state functional connectivity within and between these networks
117 was shown to predict creative abilities (54, 55) and task-based functional connectivity within and
118 between these networks increased during a creativity task, compared to a control task (5, 43). A recent
119 approach in neuroimaging research is connectome-based predictive modeling (CPM) (56), which uses
120 machine learning methods to identify patterns of functional connectivity that predict complex cognitive
121 functions, including divergent thinking ability (43, 56–61). Unlike previous research that focused on the
122 brain connectivity associated with specific creativity tasks (e.g., divergent thinking), the current study
123

124 explores the neurocognitive determinants of real-life creativity by studying the neural basis of semantic
125 memory organization related to creative behavior. We hypothesized that the associative mechanisms
126 reflected by SemNet metrics are relevant to real-life creative activities and achievements and can be
127 predicted by functional connectivity patterns, involving, in particular, the control, default, and salience
128 networks (43).

129 To this end, we first examine the organization of individual SemNets via network metrics and
130 identify the SemNet metrics that reliably predict differences in creative achievement and thus constitute
131 cognitive markers of real-life creativity. We then explore the functional connectivity of brain networks
132 predicting individual differences in these SemNet markers. We use the CPM method and analyze
133 functional brain connectivity during the performance of the semantic relatedness task that is used to
134 estimate individual SemNets. We identify the task-based functional connectivity patterns predicting
135 individual differences in SemNet properties. Finally, we examine whether SemNet properties mediate
136 the link between these brain connectivity patterns and real-life creativity, thus linking functional
137 connectivity to real-life creativity via individual differences in semantic memory organization.

138 Results

139 Individual Semantic Network metrics and creativity

140 First, we explored the properties of individuals' SemNets in relation to creativity. Similar to
141 previous studies (36–38), we estimated participants' individual semantic memory network as weighted
142 (WUN) and unweighted (UUN) SemNets based on performance in the semantic relatedness judgment
143 task (RJT; **Figure 1**). During the RJT, participants judged the relatedness between all possible pairs of
144 35 words (595 ratings). We then computed established network measures in cognitive network research
145 including (29): Average Shorter Path Length (*ASPL*; measuring average distances, or the spread of the
146 SemNet), Clustering Coefficient (*CC*; measuring overall connectivity in the SemNet), Modularity (*Q*;
147 measuring the level of segregation of the SemNet) and Small Worldness (*S*; measuring the ratio between
148 connectivity and distances in the network (62); see *Material and Methods*). In addition, we assessed
149 individual differences in real-life creative activities (*C-Act*) and achievements (*C-Ach*) via the Inventory
150 of Creative Activities and Achievements (42) completed outside the MRI scanner (Descriptive statistics
151 for behavioral and network measures are reported in **Table 1**).

152 We then examined how SemNet metrics predict real-life creativity by applying linear regression
153 models, regressing creativity on each SemNet metric with leave-one-out cross-validations: We
154 iteratively fitted predictive linear models in N-1 participants and tested the model in the left-out
155 participant. The significance of the model prediction was assessed by the correlation between the
156 predicted value of *C-Act* (or *C-Ach*) computed by the model and the observed value using permutation
157 testing. These analyses revealed that both real-life creative activities and achievements are predicted
158 from different individual SemNet metrics (**Figure 2**). The Spearman correlations showing the direction
159 and size of the relationships between SemNet metrics and creativity are reported in **Table 2**. *C-Act* was
160 predicted from WUN *ASPL* and UUN *Q*. *C-Ach* was predicted from WUN *Q* and UUN *Q*. More creative
161 individuals had less modular SemNets.

162

163 Prediction of creativity-related SemNet properties from brain connectivity

164 We applied the connectome-based predictive modeling (CPM) approach (43, 56, 57, 59) to
165 explore whether task-based functional connectivity patterns predict semantic memory network metrics
166 that related to creativity (i.e., *Q* in WUN and UUN, and *ASPL* in WUN; see **Table 2**; The applied CPM
167 approach is illustrated in **Figure 3**). We used a functional brain atlas to define 200 brain nodes belonging
168 to 17 functional networks (63). For each participant, Pearson correlations of the BOLD signal between
169 all unique pairs of brain regions (i.e., nodes; $n = 19,900$) were computed to estimate the task-related
170 functional connectivity of the whole brain connectivity network (**Figure 3a**). We then identified relevant
171 links of the brain connectivity network that positively (positive model network) or negatively (negative
172 model network) correlated with the SemNet metric across participants (**Figure 3b**). Next, we adapted
173 the classical CPM method (56) to better take into account the network properties of the brain model
174 networks. Instead of using the sum of the connectivity in the model networks, we computed two key
175 network metrics describing small-worldness properties of human brain networks (64–66): their *CC*

176 (brain-CC) and *efficiency* (brain-Eff; **Figure 3c**). We then ran six separate linear models regressing each
177 SemNet metric (Q for WUN and UUN, and *ASPL* for WUN) on each model network metric (brain-CC
178 and brain-Eff). We used leave-one-out cross-validations, iteratively fitting predictive linear models in
179 N-1 participants and tested these models on the left-out participant (**Figure 3d**). Finally, the model
180 prediction was assessed by the Spearman correlation between the predicted value from the model and
181 the observed values.

182 We then tested the relation between predicted and observed CPM models on the various SemNet
183 metrics, using 1,000 iteration permutation testing (56) (**Figure 4**). The CPM-based prediction from
184 brain-CC was significant for the WUN Q metric ($r = .386, p = .004$). The CPM-based predictions from
185 brain-Eff were significant for the WUN Q metric ($r = .476, p = .001$) and the UUN Q metric ($r = .272,$
186 $p = .036$). The CPM-based predictions of WUN *ASPL* from both brain-CC and brain-Eff, and UUN Q
187 from brain-CC were not significant, showing either a negative correlation between predicted and
188 observed values or did not reach a significant p -value after permutation testing. In summary, CPM
189 analyses on task-based functional connectivity showed that brain connectivity *CC* and *efficiency* allowed
190 reliable predictions of SemNet Q .

191
192

193 **Functional anatomy of the predictive brain connectivity patterns**

194 To characterize the functional brain connectivity patterns predictive of SemNet metrics, we
195 explored the links of the model networks that account for SemNet properties relevant to creativity.
196 Unique positive and negative model networks were identified for each SemNet metric (56) (**Figure 3b**)
197 and used to compute their network properties (brain-CC and brain-Eff; **Figure 3c**). Since SemNet
198 *modularity* (Q) was negatively correlated with both creativity measures (*C-Act* and *C-Ach*; **Table 2**) as
199 expected from previous studies (11, 36–38), we focused on the description of the negative model
200 network predicting *UUN Q* (**Figure 5**) or *WUN Q* (**SI Figure S1**). In this model network, we considered
201 the links that were shared in all iterations of the leave-one-out analysis, as the links in the model network
202 can slightly vary at each iteration.

203 For the standard CPM negative model network of *UUN Q*, we identified 452 links. Connectivity
204 of these links related to lower SemNet Q , which again predicted higher real-life creativity. These links
205 represented connections mainly within and between temporal, parietal, limbic and prefrontal lobes
206 (**Figure 5a-b**). When we explored the distribution of these links at the functional networks level, based
207 on the functional networks included in the Schaefer atlas (63), most of the links were part of the
208 somatomotor, salience and default mode networks (**Figure 5c**). The highest number of links were found
209 between control and default mode networks (8.2%), followed by links within the salience network and
210 between somatomotor and visual networks. In this model network, the highest degree nodes — nodes
211 with highest number of connections (k ; i.e., the number of functional connections) — belonged to the
212 right hemisphere being part of the visual network (i.e., extra-striate inferior, $k = 53$), default mode
213 network (i.e., medial prefrontal cortex, $k = 39$), salience (i.e., insula, $k = 31$; parietal medial, $k = 28$),
214 temporoparietal (i.e., temporal-parietal; $k = 29$) and limbic (temporal pole, $k = 28$) networks (**Figure 5d**).
215 In summary, the main patterns of functional connectivity that predicted lower SemNet Q (i.e., related to
216 higher creativity) had a whole-brain distribution and involved the control, default mode, salience and
217 somatomotor networks.

218
219

220 **Mediation Analysis**

221 In the previous analyses, we found a relationship between SemNets and real-life creativity, and
222 between brain functional connectivity and SemNets. In a final step, we analyzed whether the relationship
223 between functional brain connectivity and real-life creativity is mediated by the SemNet properties.
224 Hence, we conducted mediation analyses that focused on the indirect effect of functional connectivity
225 on creative activities and achievements, using either *C-Act* or *C-Ach* as the dependent variable for each
226 significant CPM model. To simplify interpretations, since *UUN Q* had a negative correlation with
227 creativity, its value was reversed (*UUN Q_R*) to be positively correlated with creativity.

228 Since *C-Act* was significantly predicted by the SemNet metric *UUN Q*, we explored the
229 mediating role of *UUN Q* on the relationship between the properties of the functional brain network

230 predicting UUN Q (*brain-Eff*) and *C-Act* (**Figure 6a**). As shown in the previous analyses, the regression
231 coefficient between *brain-Eff* and *UUN Q_R* was statistically significant ($\beta = .305, p < .001$), as was
232 the regression coefficient between *UUN Q_R* and *C-Act* ($\beta = .443, p = .002$). The total effect and the
233 direct effect were not statistically significant ($\beta = .116, p = .328; \beta = -.019, p = .872$). We tested
234 the significance of the indirect effect using a bootstrapping method. The bootstrapped indirect effect
235 was $(.305) * (.443) = .135$, and the 95% confidence interval ranged from 0.024 to 0.320. Thus, the indirect
236 effect was statistically significant ($p = .002$). Hence, SemNets *UUN Q* mediated the relationship between
237 the efficiency of functional brain connectivity (*brain-Eff*) and creative activities (*C-Act*): The higher the
238 efficiency of the negative model network that predicts *UUN Q*, the lower the *SemNet Q*, and the higher
239 are real-life creative activities.

240 *C-Ach* score was predicted from *SemNet WUN Q* and *UUN Q* metrics. We explored the
241 mediating role of *UUN Q* between the functional connectivity of the negative model network predicting
242 it (*brain-Eff*) and *C-Ach* (**Figure 6b**). The mediation analysis showed that the regression coefficient
243 between *brain-Eff* and *UUN Q_R* was statistically significant ($\beta = .305, p < .001$), as was the regression
244 coefficient between the *C-Ach* and *UUN Q_R* ($\beta = .241, p = .005$). The total effect and the direct effect
245 were not statistically significant ($\beta = .142, p = .056; \beta = .069, p = .353$). The bootstrapped indirect
246 effect was $(.305) * (.241) = .073$, and the 95% confidence interval ranged from 0.018 to 0.140. Thus, the
247 indirect effect was statistically significant ($p < .001$).

248 Hence, SemNets *UUN Q* mediated the link between the efficiency of brain functional
249 connectivity (*brain-Eff*) and real-life creative achievements (*C-Ach*): The higher the efficiency of the
250 negative model network that predicts *UUN Q*, the lower the *modularity* of *SemNet*, and the higher the
251 real-life creative achievements.

252 Similarly, we explored the mediating role of *WUN Q* on the relationship between the properties
253 of the functional connectivity of the negative model network predicting it (*brain-Eff* and *brain-CC*) and
254 *C-Ach* (**Figure 6c**). Using *brain-Eff* as an independent variable, the regression coefficient between
255 *brain-Eff* and *WUN Q_R* was significant ($\beta = .286, p = .004$), as was the regression coefficient between
256 *C-Ach* and *WUN Q_R* ($\beta = .183, p = .015$). The total effect and the direct effect were not statistically
257 significant ($\beta = .094, p = .183; \beta = .042, p = .560$). The bootstrapped indirect effect was
258 $(.286) * (.183) = .052$, and the 95% confidence interval ranged from 0.005 to 0.110. Thus, the indirect
259 effect was statistically significant ($p = .018$).

260 Using *brain-CC* as independent variable, the regression coefficient between *brain-CC* and *WUN Q_R* was significant ($\beta = .280, p = .008$), as was the regression coefficient between *C-Ach* and *WUN Q_R* ($\beta = .192, p = .01$) (**Figure 6d**). The total effect and the direct effect were not statistically
261 significant ($\beta = .068, p = .365; \beta = .014, p = .850$). The bootstrapped indirect effect was
262 $(.280) * (.192) = .054$, and the 95% confidence interval ranged from 0.006 to 0.130. Thus, the indirect
263 effect was statistically significant ($p = .018$).

264 Hence, *SemNet WUN Q* mediated the link between the efficiency (*brain-Eff*) and the clustering
265 coefficient (*brain-CC*) of functional brain connectivity and real-life creative achievements (*C-Ach*): The
266 higher the efficiency and clustering of the negative model network that predicted *WUN Q*, the lower
267 *SemNets Q*, and the higher the real-life creative achievements. In summary, individual *SemNets Q*
268 measured in *WUN* and *UUN* networks mediated the relationship between brain functional connectivity
269 and real-life creativity.

270

273 Discussion

274

275 Our results provide a new neuroscientific understanding of the individual determinants of real-
276 life creative behavior. Recently developed computational approaches allowed us to predict complex
277 cognitive functions from brain connectivity (56–58) and to explore the organization of semantic memory
278 at the individual level using SemNets (36–38). The unprecedented combination of these approaches
279 revealed unique patterns of brain functional connectivity that reliably predict differences in real-life
280 creativity via semantic network structure. Using the CPM approach, we show that brain connectivity
281 during semantic relatedness judgments predicted individual differences in the *modularity* (*Q*) of
282 SemNets that was identified as a behavioral marker of creativity. Specifically, the efficiency and

283 clustering of whole-brain connectivity patterns predicted differences in real-life creativity mediated by
284 *SemNet modularity*.

285 According to the associative theory of creativity ⁷, high creative individuals are characterized
286 by a more flexible organization of concepts in their semantic memory, allowing them to retrieve remote
287 associations more easily (14, 16). A recent study revealed the mediating role of associative abilities
288 between semantic memory structure and creativity as measured by verbal creativity but not by figural
289 creativity (38). Here, we show that individual semantic memory network properties also relate to real-
290 life creativity: individuals with a more compact and less modular organization of their semantic memory
291 exhibit higher creative activities and achievements. This finding is consistent with previous studies
292 reporting a strong relationship between semantic associative ability and creative behavior in real-life
293 (27, 28). It suggests that this relationship may be explained by individual differences in semantic
294 memory structure. We showed that *SemNet modularity* represents both a behavioral marker of real-life
295 creativity and a mediating mechanism underlying the effect of brain functional connectivity on real-life
296 creative activities and achievements. The higher the efficiency and overall connectivity of the brain
297 predictive network, the more flexible the semantic network (characterized by being more compact and
298 less modular), and the more creative the participant is. This result is in line with previous studies (11,
299 36, 37) and suggests that more creative individuals have better access to remote concepts within their
300 semantic memory than less creative individuals (8, 10). Importantly, higher modularity in linguistic
301 networks has been linked to rigidity (67) and inefficient conceptual processing (68). Thus, less modular
302 networks allow more flexible thinking, with a higher connectivity between weakly related elements
303 facilitating their combination.

304 Previous studies exploring the cognitive processes involved in creativity have revealed brain
305 regions and functional networks associated with different creativity tasks (5, 44, 45). The use of
306 SemNets allowed us to explore cognitive mechanisms that appear more broadly relevant to associative
307 basis of creative cognition, avoiding the specificities of existing tasks. Using a whole-brain functional
308 connectivity approach, we identified the task-based functional connectivity patterns related to semantic
309 network properties predicting real-life creativity (activities and achievements). These patterns included
310 functional connections distributed across the whole brain, the densest being observed between brain
311 networks previously linked to creativity (5, 43, 53, 69–71). The major contributions to the prediction of
312 creativity resulted from functional links between control and default mode network, within salience
313 network, and between somatomotor and visual networks. The default mode network has been
314 consistently associated with self-generated thought and spontaneous associations (16, 19, 72, 73). In
315 contrast, the control network is associated with controlled processes such as attentional control, working
316 memory, inhibition, memory retrieval, and flexibility, which are necessary to accomplish the objectives
317 of a specific task (15, 74, 75). The functional coupling between control and default mode networks has
318 been reported in relation to creative cognition in several studies using different approaches such as
319 verbal divergent thinking tasks (5, 69), musical improvisation (76), poetry composition (77) and visual
320 arts (78).

321 In addition to control and default mode network, the salience network has also been reported to
322 play a critical role in creativity. It has been associated with attentional switching and detection of salient
323 external or internal stimuli and appears to play a role in triggering the engagement of control and default
324 mode networks during creativity tasks (69, 79). Overall, our finding converges with previous
325 correlational (5, 69) and predictive studies of creativity using CPM approach (43, 58) indicating the
326 essential role of the functional connectivity within and between control, default and salience networks
327 for creative thinking abilities.

328 A considerable number of functional connections between somatomotor and visual networks
329 also contributed to the prediction of creativity via *SemNet* properties. Both networks have been
330 associated with creativity in previous studies (53, 70, 80, 81), but independently. The motor system has
331 been related to creativity (53, 82) as measured by different approaches, including verbal creativity (71),
332 music improvisation (80, 81, 83), and visuospatial creativity (70, 71). The brain regions of visual
333 networks also appear to play an important role mainly in artistic creativity (71) and their activation was
334 previously correlated with higher creative achievements (84). A recent study using the CPM approach
335 showed the contribution of visual networks in the overlapping brain patterns predicting creativity and
336 intelligence (58). Our study adds to this previous work by showing the involvement of the coupling of
337 motor and visual networks in creativity. The role of motor and visual regions in creativity can be plural.

338 In the context of our RJT task used to estimate SemNets, semantic relatedness judgments may evoke
339 visual representations and motor experiences associated with the concepts (85). It is then possible that
340 less modular SemNets reflect less segregated motor and visual memory contents in higher creative
341 individuals than in less creative ones, and closer connections between remote concepts in memory.

342 Overall, our finding further supports and expands existing knowledge on the functional
343 interaction within and between control, default mode and salience networks for creativity (43) by
344 showing their link with real-life creativity and characterizing their role in the associative mechanisms
345 captured by SemNet metrics. In addition, the current findings shed light on the contribution of the
346 increased coupling between regions of the visual and motor networks for creativity.

347 To further characterize the predictive patterns of functional brain connectivity, we identified the
348 nodes with the highest number of connections being localized in the medial prefrontal cortex, insula, the
349 extra-striate inferior region, parietal medial and temporoparietal regions, and temporal pole in the right
350 hemisphere. Most of these regions have been reported to play a role in creative cognition. In a brain
351 lesion study, the medial prefrontal cortex of the default mode network has been shown to be relevant in
352 associative processes underlying creative cognition (16). Moreover, this brain region and the insula of
353 the salience network have been highlighted as essential regions for verbal creativity (5, 43, 86). The
354 right lingual gyrus, part of the extra-striate cortex, is also recruited in verbal creativity tasks (44, 45) in
355 relation to the originality of semantic associations (28), and to internally directed attention reflecting
356 increased visual imagery (87). Other temporal areas, including the right temporoparietal regions and
357 temporal pole have been associated with verbal and visual creativity (45, 88), including insight problem
358 solving (89), and mental imagery (90). The involvement of the anterior temporal pole is consistent with
359 its role as a semantic hub (85, 91, 92) and in abstract thinking and categorization (93, 94).

360 One surprising result is that the highest degree brain nodes related to real-life creativity were
361 distributed within the right hemisphere. Previous analyses reported a left dominance for creativity
362 regions in functional (44, 45, 50), connectivity (43), and structural (95) imaging studies. Most verbal
363 creativity tasks highlight the critical role of brain regions of the left hemisphere, particularly in the
364 prefrontal and temporal cortex, possibly related to linguistic/semantic processing (44, 96, 97). Here, we
365 also identified left-sided highly connected nodes contributing to the prediction of differences in real-life
366 creativity in the left ventral prefrontal cortex of the control network and in the insula of the salience
367 network, regions that have been shown critical for verbal creativity (44, 45, 98, 99). Yet, the right
368 dominance of the predictive patterns in our study was unexpected because our study focused on the
369 semantic basis of creative cognition and used a verbal task. The strong engagement of the right
370 hemisphere might be related to the process of judging remote concepts during the RJT. Previous studies
371 have indeed associated the right hemisphere with a relatively coarser semantic coding (100) and the
372 activation of broader semantic fields by words or contexts (101). Moreover, the engagement of broad
373 associative processes in the right hemisphere has been related to hemispheric brain asymmetries in
374 dopamine function (102). More creative individuals may rate distant words as more related during the
375 RJT than less creative ones, which might rely on a higher functional connectivity with or within the
376 right hemisphere. Hence, these findings show that diverse regions previously reported as central to
377 creative cognition participate together in the predictive connectivity patterns of real-life creativity
378 through a less segregated organization of semantic memory (lower SemNet *modularity*). Whether and
379 how SemNet *modularity* reflects remote thinking that would rely more specifically on the right
380 functional connectivity remain to be addressed in future studies.

381 Finally, the current SemNets-related results converge with and expand the few recent
382 neuroimaging studies exploring the associative processes of creativity. Higher associative abilities in a
383 free chain association task have been related to higher resting-state functional connectivity within the
384 default mode network (19) and to larger gray matter volume in the left posterior inferior temporal gyrus
385 (49). In both studies, higher associative abilities mediated the relationship between a priori selected
386 regions of the brain and creativity. One recent study showed that efficiency in SemNets mediated the
387 link between gray matter volume in the left temporal pole and a divergent thinking task (41). Our
388 findings advance this knowledge in several critical ways. First, by using SemNets, we were able to
389 estimate the organization of semantic memory, which offers some mechanistic perspective on remote
390 and associative thinking, and showed its role in real-life creativity. Second, we employed a whole brain
391 approach without focusing on a priori regions or networks. Finally, we explored functional connectivity
392 not during rest, but during the RJT, while all participants performed the same trials. This approach

393 minimized individual differences in mental activity during scanning. It importantly gave access to the
394 functional connectivity configuration that occurs during semantic relatedness judgments that reflect
395 semantic associations.

396 Some limitations to this study need to be acknowledged. First, our sample is relatively small
397 and although the results are robust, the use of additional external validation would add strong support to
398 our findings. Second, we used the SemNet approach that is rooted in the associative theory of creativity
399 (7) to estimate individual semantic memory networks based on relatedness judgments of word pairs.
400 The RJT-based SemNet metrics may not capture all the complexity of associative thinking. Thus, future
401 studies are needed to replicate our findings, using alternative methods to estimate individual's SemNets.
402 How the results generalize across different creative performances and behaviors, in distinct domains,
403 also remains to be explored. Finally, real-life creativity is not exclusively predicted by semantic
404 memory. Many other internal and external factors are important to creativity, such as personality,
405 motivation, emotions and environment (1, 2, 103–106). Despite these other potential dimensions and
406 sources of variability, the brain connectivity patterns allowed us to predict real-life creativity through
407 the individual differences in semantic memory structure, suggesting its strong influence on creative
408 activities and achievements.

409 In conclusion, the current findings uniquely link brain functional connectivity, semantic
410 memory structure, and real-life creativity by combining advanced network-based methods in novel
411 ways. By exploring semantic memory organization using SemNet methods, we were able to predict
412 creative abilities independently of narrow frameworks or tasks. Our connectome-based modeling
413 approach identified brain connectivity patterns that predicted creative behaviors rooted in semantic
414 memory properties. By converging these two approaches together, our study illustrates how the network
415 organization of the brain and of memory can be related to each other, leading to exciting new frontiers
416 of scientific inquiry.

417
418

419 Materials and Methods

420 Participants

421 All participants were French native speakers, right-handed, with normal or corrected-to-normal
422 vision and no neurological disorder, cognitive disability or medication affecting the central nervous
423 system. One hundred one healthy participants (48 women) aged between 22 and 40 years (mean $25.6 \pm$
424 SD 3.7) were recruited via the RISC platform (<https://www.risc.cnrs.fr>). In total, eight participants were
425 excluded from the fMRI analysis: Six were excluded because of the discovery of MRI brain
426 abnormalities, one fell asleep during the acquisition of the data, and another had a claustrophobia
427 episode at the beginning of the MRI scanning. The latter participant performed the RJT task outside the
428 scanner and was kept in the behavioral analyses only. The final sample was hence composed of 94
429 participants aged between 22 and 37 years (mean 25.4 ± 4.2) in behavioral analyses and 93 participants
430 in the fMRI analyses (mean age 25.4 ± 3.4 ; 44 women). A national ethical committee approved the
431 study. After being informed of the study, the participants signed a written consent form. They received
432 monetary compensation for their participation.

433

434 **General procedure**

435 Participants underwent a task-based fMRI session during which they performed the Relatedness
436 Judgment Task (RJT). Several training tasks were conducted before acquiring the fMRI data, first
437 outside the scanner, then in the scanner. The training included a motor training task to become familiar
438 with giving responses using the MRI-compatible trackball on a visual scale in the RJT, and a task
439 training to get familiar with the actual task. The task training was similar to the actual task but using
440 different stimuli. In addition, all words used in the RJT were displayed to participants to check that they
441 were familiar with all of them (Details of the task training are described in **SI S1**). After the fMRI
442 session, participants completed a set of creativity tasks on a computer outside the scanner that lasted
443 around three hours.

444

445 **Relatedness judgement task (RJT)**

446 **Task and material description**

447 The RJT has been used to estimate individual-based SemNets and to explore the structure of
448 semantic memory (36–38). The task requires participants to judge the relatedness of all possible pairs
449 of words from a list of cue words. These judgements are then used to estimate an individuals' semantic
450 memory network of these words. The selection of the RJT stimuli words used in our study is detailed in
451 Bernard et al. (37). In brief, we first created a French SemNet, based on French verbal association norms
452 (107) (<http://dictaverf.nsu.ru/dictlist>), where the nodes represent the words, and the links were weighted
453 by the normative associative strength between words. Next, we computed the shortest path between
454 words and the minimal number of links between each pair was considered as the theoretical semantic
455 distance between the words. Finally, we applied a computational method to select the RJT words that
456 optimized the repartition of the theoretical semantic distance between all possible pairs of these words.
457 The optimal solution included 35 words, resulting in a total of 595 word-pairs that represented the 595
458 RJT trials.

459 Each trial began with the displaying word pair on the screen along with a visual scale below
460 ranging from 0 (unrelated) to 100 (strongly related). The stimuli were displayed for 4 seconds in total,
461 divided into a reflection period of 2 seconds to ensure a comparable minimum judgement time and a
462 response period of 2 seconds. During the first two seconds, the participants studied the word pair but
463 couldn't move the slider yet. Two seconds after stimuli onset, the response period began, the cursor
464 appeared in the middle of the visual scale, and the participants were allowed to move the slider on the
465 visual scale to indicate their rating using a trackball. Participants were instructed to validate their
466 response by clicking the left button of the trackball. The position of the cursor on the scale at the moment
467 of the validation was recorded as the relatedness judgment. When participants did not validate their
468 response, we recorded the slider position at the end of the two-second response period. After the
469 response period, a blank screen was shown during the inter-trial interval jittered from 0.3 to 0.7 seconds
470 (steps = 0.05; **Figure 1a**).

471 Task trials were distributed into six runs composed of 100 trials each, except for the last run (95
472 trials). Each run consisted of four blocks of 25 trials each (except the last block of the sixth run with
473 only 20 trials), separated by a 20 second rest period with a cross fixation on the screen. Trials were
474 pseudo-randomly ordered within blocks, such that each block contained a similar proportion of word
475 pairs of each theoretical semantic distance. At the beginning and end of each run, participants had a ten
476 second rest period with a cross fixation on the screen. During the last two seconds of fixation cross
477 periods, the cross changed color, warning the participant that the task was about to start. Participants
478 had a self-paced break inside the scanner between runs.

479

480 **Assessment of individual semantic network structure.**

481 ***Building individual semantic networks***

482 The relatedness ratings given by the participant to each pair of words was used to weight the
483 links of the individual SemNet where each word is a node. We represent each of these networks as a
484 35x35 matrix with one column and one row for each word and cell values correspond to the judgment
485 given by the participant during the RJT task (**Figure 1b**). Based on previous studies and on our pilot
486 study (36–38), we estimated two types of networks, weighted undirected network (WUN) and

487 unweighted undirected network (UUN; **Figure 1c**). The WUN is a more conservative type of the
488 SemNet, by keeping the weights of all links between the words. The UUN is a less conservative
489 approach, retaining links above a defined threshold, and the links with a weight below the threshold are
490 removed. We defined the threshold as rating value of 50 (the middle of the visual scale) to keep the links
491 between words that were considered moderately or highly associated by the participants. The weights
492 of the remaining links are uniformly transformed to equal 1.

493

494

495 *Calculation of the individual semantic network metrics*

496 We estimated the properties of the individual SemNet independently for the UUN and the WUN
497 graphs. Based on previous studies relating SemNet to creative abilities (11, 34, 36–38), we computed
498 the following metrics: *ASPL*, *CC*, *Q* and *S* metrics. The Average Shortest Path Length (*ASPL*) is the
499 average shortest number of steps needed to be taken between any pair of nodes. In semantic networks,
500 path length reflects how related two concepts are to each other (108, 109). The Clustering Coefficient
501 (*CC*) measures the network's connectivity. It refers to the probability that two neighbors of a node will
502 themselves be neighbors. In semantic networks, higher *CC* relates to higher overall relatedness between
503 concepts. Modularity (*Q*) measures how a network is divided (or partitions) into smaller sub-networks;
504 a higher *Q* relates to more sub-communities in the network (110, 111). Such subcommunities can reflect
505 semantic categories in a semantic network. In creativity research, for example, more creative individuals
506 often exhibit a more connected (higher *CC*), less segregated (lower *ASPL* and *Q*) semantic network than
507 less creative individuals ³⁴ and these differences were related to flexibility of thought (35). The small-
508 worldness (*S*) property of the network is calculated as the ratio between *ASPL* and *CC* and describes
509 how much the nodes that are not directly linked can be reached through connections between their
510 neighbors. In semantic networks, higher *S* has been linked to higher flexibility of thought (11). The
511 computations were performed in Matlab, via the Brain Connectivity Toolbox (112)
512 (<https://www.mathworks.com>).

513

514 *Assessment of real-life creativity*

515 Outside the scanner, we used the Inventory of Creative Activities and Achievements (*ICAA*)
516 questionnaire (42) to assess the real-life creative activities and achievements across eight different
517 creative domains (e.g., literature, music, art and crafts, cooking, sport, visual arts, performing arts,
518 science and engineering). The creative activities (*C-Act*) score reflects the frequency in which
519 participants engaged in various creative activities. Six different questions were posed for each domain,
520 and participants reported the frequency with which they engaged in each activity during the last ten
521 years, using a scale ranging from 0 (never) to 4 (more than ten times). For each participant, the final
522 domain-general score of *C-Act* was the sum of the creative activities across all activities of the eight
523 different domains. The creative achievements (*C-Ach*) score estimated the level of achievement acquired
524 in a creative domain. Ten different levels of achievement were included for each domain going from 0
525 (never engaged in this domain) to 10 (I have already sold some of my work in this domain). For each
526 participant, the final domain-general score of *C-Ach* was the sum of the scores across the eight different
527 domains.

528

529 *Relationships between individual Semantic Network metrics and creativity*

530 We explored whether individual SemNet properties were predictive of real-life creative
531 activities (*C-Act*) and achievements (*C-Ach*; **Figure 1e**). In independent analyses, we performed linear
532 regressions using leave-one-out cross-validations to predict *C-Act* and *C-Ach* scores for each of the
533 SemNet metrics (*ASPL*, *CC*, *Q*, and *S* of WUN and UUN SemNets). The analyses consisted of building
534 a predictive linear model iteratively in N-1 participants using their SemNet metrics (e.g., WUN *Q*
535 SemNet metric) and testing it in the left-out participant. The model was applied on the SemNet metric
536 of the left-out participant to compute a predicted value of the ICAA scores. The significance of the
537 prediction was evaluated via Spearman correlations between the predicted and the observed creativity
538 scores. When the correlations between observed and predicted values were positive with $p < .05$, we
539 assessed its statistical significance using 1,000 iteration permutation testing. We report the Rho
540 coefficient and the *p*-value of the permutation test. Note that Spearman correlations are used for

541 behavioral analyses as creative activities and achievements are typically skewed (113). We also ran
542 Spearman correlations between SemNet metrics and ICAA scores to better represent the statistical
543 association between the different SemNet metrics and creativity (**Table 1**).
544

545 MRI Data Acquisition and Preprocessing

546 Neuroimaging data were acquired on a 3T MRI scanner (Siemens Prisma, Germany) with a 64-
547 channel head coil. Six functional runs were acquired during each six task runs using multi-echo echo-
548 planar imaging (EPI) sequences. No dummy scan was recorded during the acquisition; therefore, we did
549 not discard any volume. Each run included 335 whole-brain volumes acquired with the following
550 parameters: repetition time (TR) = 1,600 ms, echo times (TE) for echo 1 = 15.2 ms, echo 2 = 37.17 ms
551 and echo 3 = 59.14 ms, flip angle = 73°, 54 slices, slice thickness = 2.50 mm, isotropic voxel size 2.5
552 mm, Ipat acceleration factor = 2, multi-band = 3 and interleaved slice ordering. After the EPI
553 acquisitions, a T1-weighted structural image was acquired with the following parameters: TR = 2,300
554 ms, TE = 2.76 ms, flip angle = 9°, 192 sagittal slices with a 1 mm thickness, isotropic voxel size 1 mm,
555 Ipat acceleration factor = 2 and interleaved slice order. A resting state fMRI session of 15 minutes
556 followed, not analyzed in the current study.

557 The preprocessing of the on-task fMRI data was performed for each run separately using the
558 afni_proc.py pipeline from the Analysis of Functional Neuroimages software (AFNI;
559 <https://afni.nimh.nih.gov>) (114). The different preprocessing steps of the data included despiking, slice
560 timing correction and realignment to the first volume (computed on the first echo). We then denoised
561 the preprocessed data using the TE-dependent analysis of multi-echo fMRI data (TEDANA;
562 <https://tedana.readthedocs.io/en/stable/>), version 0.0.9 (115–117). The advantage of using multi-echo
563 EPI sequences is that it allows better cleaning of the data by assessing the BOLD and non-BOLD signal
564 through the ICA-based denoising method, improving the reliability of the functional connectivity-based
565 measurement (118). The TEDANA pipeline consisted first of an optimal combination of the different
566 echo time series. Then, the dimensionality of the optimally combined data is reduced through the
567 decomposition of the multi-echo BOLD data using principal component analysis (PCA) and
568 independent component analysis (ICA). TEDANA then classifies the resulting components as BOLD
569 or non-BOLD. The exclusion of the non-BOLD components allowed the removal of thermal and
570 physiological noise such as the artefacts generated by the movements, respiration and cardiac activity.
571 The resulting denoised data was co-registered on the T1-weighted structural image using the Statistical
572 Parametric Mapping (SPM) 12 package running in Matlab (Matlab R2017b, The MathWorks, Inc.,
573 USA). We then normalized the data to the Montreal Neurological Institute (MNI) template brain, using
574 the transformation matrix computed from the normalization of the T1-weighted structural image,
575 performed with the default settings of the computational anatomy toolbox (CAT 12;
576 <http://dbm.neuro.uni-jena.de/cat/>) (119) implemented in SPM 12. The resulting denoised and
577 normalized images were then entered in a general linear model (GLM) in SPM to covary out the task-
578 related signal from each run. In this analysis, we entered 24 motion parameters (standard motion
579 parameters, first temporal derivatives, standard motion parameters squared and first temporal derivatives
580 squared) and the onsets and durations of each task related events (reflection period, response period,
581 inter trial interval, cross fixation periods and change of the cross-fixation color) as confounds that were
582 regressed from the BOLD signal. We standardized and detrended the residuals of this model for each
583 run and then concatenated the six runs, removing the rest periods between runs (six volumes in total).
584 This final dataset composed of the six task-run residuals concatenated was used as input for the
585 subsequent task-based functional connectivity analyses.
586

587 Building task-based functional connectivity matrices

588 Calculation of the task-based functional connectivity matrices for each participant was
589 performed using Nilearn v0.3 (120) in Python 2.7 (121). We used the Schaefer brain atlas to define our
590 ROIs that consisted of 200 ROIs distributed into 17 functional subnetworks than can be summarized in
591 eight main functional networks (63). For each ROI, we extracted the BOLD signal during the RJT
592 (averaged across voxels) and computed Pearson correlation coefficients of all pairs of ROIs. As a result,
593 we obtained for each participant a 200x200 matrix with the correlation coefficients between all ROIs.
594 These matrices were Z-Fisher-transform and rescaled in the range of -1 to 1 for the subsequent analyses.

595 This matrix corresponds to the functional connectivity network of each participant in which ROIs are
596 the nodes and correlation coefficients the links.
597

598 A connectome-based predictive modeling approach

599 We used a CPM approach (43, 56, 57, 59) to explore how SemNet properties can be predicted
600 from functional connectivity patterns during the RJT task. We focused the CPM analyses on the SemNet
601 metrics that predicted creativity scores following the method described in Shen et al. (56) (**Figure 3**).
602 We used a leave-one-out cross-validation that consisted in building the model iteratively on N-1
603 participants and test the prediction on the left-out participants.

604 Since head motions during the fMRI acquisition can affect the CPM results, we verified that
605 there was no correlation between motion patterns during the fMRI acquisition and the SemNet metrics.
606 We estimated the mean FD, that is the sum of the absolute values of the derivatives of the six realignment
607 parameters (122), and computed Spearman correlations between the mean FD and all SemNet metrics.
608 The correlations revealed no significant correlation between the motion patterns and WUN *ASPL* ($r = -.052, p = .622$), WUN *Q* ($r = .133, p = .203$) and UUN *Q* ($r = .127, p = .225$).

609 The first step of the CPM consists of selecting the significant features of brain connectivity to
610 build the "model brain networks". In the training set ($N-1$), we selected the links of the functional
611 connectivity matrix (correlation coefficients between the ROIs) that significantly correlated with the
612 tested SemNet metric (threshold $p < .05$) either positively (the positive model network) or negatively
613 (the negative model network) across participants (**Figure 3a-b**). Since SemNet metrics had non-
614 Gaussian distributions, we used Spearman correlations. In these model networks of brain connectivity,
615 negative links were removed (123). We normalized the values of the links (i.e., the correlation
616 coefficients between ROIs) to have the same range of values for the calculation of the brain networks in
617 the following step.

618 The second step consists in estimating functional connectivity properties within each
619 participant's positive and negative model networks. This is one amendment from the classical protocol
620 (56) to better take into account the structural properties of functional brain connectivity patterns. Instead
621 of summing the links in the model networks (as in the classical CPM method), we estimated the network
622 properties of the positive and the negative model networks using network metrics (**Figure 3c**). We
623 computed two different whole-brain model network metrics: 1) Network efficiency (*brain-Eff*),
624 measuring rapid and efficient integration across the network (69, 124) and 2) *CC* (*brain-CC*), key
625 property describing a small-world properties network characterizing the human brain (64, 65, 125–127).
626 The *brain-Eff* metric was calculated as the average of the inverse shortest path length. The computation
627 of the *brain-CC* metrics was similar to the *CC* of the SemNet described above in the "Calculation of the
628 individual semantic network metrics" section.

629 The third and fourth steps consist in building the predictive model using the computed network
630 properties and then applying it to a novel participant (the left out one for each iteration; **Figure 3d**).
631 These steps were conducted separately for each SemNet metric and each model network property. We
632 built a single linear model combining the network metric of the positive and negative model networks
633 of $N-1$ participants as predictors of a given SemNet metric. The mean FD was included in the model to
634 deal with possible effects of the head motion related to fMRI acquisition on the CPM process. At each
635 iteration, we computed the network metric of the positive and the negative model networks in the left-
636 out participant. We used these values as predictors in the linear model to compute its predicted value of
637 the SemNet metric tested.

638 The final step evaluated the predictive model by performing a Spearman correlation between
639 the predicted and the observed SemNet metric (56). Since we used within-data set cross-validation, for
640 the significant predictions, it was necessary to evaluate the predictive power of the CPM using
641 permutation testing to assess the statistical significance of the results. To this end, we randomly shuffled
642 the values of the SemNet metric 1,000 times, and we ran the new random data through the pipeline of
643 our predictive model in order to generate an empirical null distribution and estimate the distribution of
644 the test statistic given by the correlation between predicted and observed values. The CPM analyses
645 were performed using Matlab Statistical Toolbox (Matlab R2020a, The MathWorks, Inc., USA). The
646 pipeline for the CPM is an adaptation from the protocol by Shen et al. (56).

649 Functional anatomy of the predicting brain model networks

650 To explore the patterns of connectivity predicting the SemNet metrics, we characterized the
651 main nodes and links of the significant model networks. We examined the distribution of the connections
652 at the lobar level (between and within brain lobes) and at the intrinsic network level (within and between
653 the eight main functional networks defined by the Schaefer atlas). Finally, we explored the brain
654 distribution of the six highest degree nodes (i.e., ROIs), which are the nodes with the highest number of
655 connections. Due to the nature of the cross-validation approach (running one model for each iteration
656 on N-1 participants), each iteration likely resulted in slightly different links in the model networks.
657 Therefore, we considered the links that were shared between all iterations. The data visualization and
658 plots were performed using BioImage Suite Web 1.0 (<http://bisweb.yale.edu/connviewer>), BrainNet
659 viewer (128) (<http://www.nitrc.org/projects/bnv/>) in Matlab, and custom scripts in RStudio
660 version 1.3.1056.

661

662 Mediation Analysis

663 To test whether the patterns of functional connectivity that predict SemNet properties are also
664 relevant for real-life creativity, we ran mediation analyses. For significant CPM predictions, we tested
665 whether the SemNet metrics mediated the relationship between the patterns of brain functional
666 connectivity and creativity. As for the CPM analyses, the mediation analyses focused on the SemNet
667 metrics that correlated with creativity scores. Hence, they explored an indirect effect of the functional
668 brain connectivity on creativity through the SemNet properties.

669 The mediation analysis (129–131) consisted in calculating the product of (a) the regression
670 coefficient of the regression analysis on the independent variable (i.e., brain functional connectivity
671 metric, *brain-CC* or *brain-Eff* of the positive or the negative model networks) to predict the mediator
672 (i.e., SemNet metrics) and (b) the regression coefficient of the regression analysis on the mediator to
673 predict the dependent variable (i.e., creativity score), when controlling for the independent variable. We
674 also calculated the regression coefficient of the regression analysis on the independent variable to predict
675 the dependent variable without controlling for the mediator (total effect) and when controlling for it
676 (direct effect; **Figure 6**). All the variables entered in the mediation analyses were normalized, and
677 variables with non-normal distributions were log-transformed. The variables that had a negative
678 correlation with creativity were reversed (multiplied by -1). The selection of the positive or the negative
679 network to be used on the mediation analysis depended on which of them is expected to be positively
680 correlated to the creativity score. We tested the significance of the indirect effect using bootstrapping
681 method, computing unstandardized indirect effects for each 5,000 bootstrapped samples, and the 95%
682 confidence interval was computed by determining the indirect effects at the 2.5th and 97.5th percentiles.
683 The mediation analyses were performed using the PROCESS macro (132) in SPSS 22.0 (IBM Corp. in
684 Armonk, NY, USA).

685

686

687 References

- 688 1. A. Lopez-Persem, T. Bieth, S. Guiet, M. Ovando-Tellez, E. Volle, Through thick and thin:
689 changes in creativity during the first lockdown of the Covid-19 pandemic. (2021),
690 doi:10.31234/osf.io/26qde.
- 691 2. T. Lubart, C. Mouchiroud, S. Tordjman, F. Zenasni, *Psychologie de la créativité - 2e édition*
692 (Armand Colin, Paris, 2e édition., 2015).
- 693 3. S. Mastria, S. Agnoli, M. Zanon, T. Lubart, G. E. Corazza, in *Exploring Transdisciplinarity in*
694 *Art and Sciences*, Z. Kapoula, E. Volle, J. Renoult, M. Andreatta, Eds. (Springer International
695 Publishing, Cham, 2018; https://doi.org/10.1007/978-3-319-76054-4_1), pp. 3–29.
- 696 4. A. Dietrich, The cognitive neuroscience of creativity. *Psychon. Bull. Rev.* **11**, 1011–1026 (2004).
- 697 5. R. E. Beaty, M. Benedek, P. J. Silvia, D. L. Schacter, Creative Cognition and Brain Network
698 Dynamics. *Trends Cogn. Sci.* **20**, 87–95 (2016).
- 699 6. P. T. Sowden, A. Pringle, L. Gabora, The shifting sands of creative thinking: Connections to
700 dual-process theory. *Think. Reason.* **21**, 40–60 (2015).
- 701 7. S. A. Mednick, The associative basis of the creative process. *Psychol. Rev.* **69**, 220–232 (1962).
- 702 8. E. Rossmann, A. Fink, Do creative people use shorter associative pathways? *Personal. Individ.*
703 *Differ.* **49**, 891–895 (2010).
- 704 9. R. E. Beaty, P. J. Silvia, E. C. Nusbaum, E. Jauk, M. Benedek, The roles of associative and
705 executive processes in creative cognition. *Mem. Cognit.* **42**, 1186–1197 (2014).
- 706 10. M. Benedek, A. C. Neubauer, Revisiting Mednick's Model on Creativity-Related Differences in
707 Associative Hierarchies. Evidence for a Common Path to Uncommon Thought. *J. Creat. Behav.*
708 **47**, 273–289 (2013).
- 709 11. Y. N. Kenett, D. Anaki, M. Faust, Investigating the structure of semantic networks in low and
710 high creative persons. *Front. Hum. Neurosci.* **8** (2014), doi:10.3389/fnhum.2014.00407.
- 711 12. E. Volle, in *The Cambridge Handbook of the Neuroscience of Creativity* (Editors: R.E. Jung and
712 O. Vartanian, New York:, Cambridge University Press., 2017), *Cambridge Handbooks in*
713 *Psychology*.
- 714 13. D. Bendetowicz, M. Urbanski, C. Aichelburg, R. Levy, E. Volle, Brain morphometry predicts
715 individual creative potential and the ability to combine remote ideas. *Cortex J. Devoted Study*
716 *Nerv. Syst. Behav.* **86**, 216–229 (2017).
- 717 14. M. Benedek, T. Könen, A. C. Neubauer, Associative abilities underlying creativity. *Psychol.*
718 *Aesthet. Creat. Arts.* **6**, 273–281 (2012).
- 719 15. M. Benedek, E. Jauk, in *The Oxford Handbook of Spontaneous Thought: Mind-Wandering,*
720 *Creativity, and Dreaming* (2018).
- 721 16. D. Bendetowicz, M. Urbanski, B. Garcin, C. Foulon, R. Levy, M.-L. Bréchemier, C. Rosso, M.
722 Thiebaut de Schotten, E. Volle, Two critical brain networks for generation and combination of
723 remote associations. *Brain J. Neurol.* **141**, 217–233 (2018).

724 17. T. Paulin, D. Roquet, Y. N. Kenett, G. Savage, M. Irish, The effect of semantic memory
725 degeneration on creative thinking: A voxel-based morphometry analysis. *NeuroImage*. **220**,
726 117073 (2020).

727 18. M. P. Ovando-Tellez, T. Bieth, M. Bernard, E. Volle, The contribution of the lesion approach to
728 the neuroscience of creative cognition. *Curr. Opin. Behav. Sci.* **27**, 100–108 (2019).

729 19. T. R. Marron, E. Berant, V. Axelrod, M. Faust, Spontaneous cognition and its relationship to
730 human creativity: a functional connectivity study involving a chain free association task.
731 *NeuroImage*, 117064 (2020).

732 20. C. S. Lee, D. J. Therriault, The cognitive underpinnings of creative thought: A latent variable
733 analysis exploring the roles of intelligence and working memory in three creative thinking
734 processes. *Intelligence*. **41**, 306–320 (2013).

735 21. R. E. Beaty, D. C. Zeiten, B. S. Baker, Y. N. Kenett, Forward Flow and Creative Thought:
736 Assessing Associative Cognition and its Role in Divergent Thinking. *Think. Sci. Creat.*, 100859
737 (2021).

738 22. M. T. Mednick, S. A. Mednick, C. C. Jung, Continual association as a function of level of
739 creativity and type of verbal stimulus. *J. Abnorm. Psychol.* **69**, 511–515 (1964).

740 23. A. E. Green, D. J. M. Kraemer, J. A. Fugelsang, J. R. Gray, K. N. Dunbar, Neural correlates of
741 creativity in analogical reasoning. *J. Exp. Psychol. Learn. Mem. Cogn.* **38**, 264–272 (2012).

742 24. A. E. Green, K. A. Spiegel, E. J. Giangrande, A. B. Weinberger, N. M. Gallagher, P. E.
743 Turkeltaub, Thinking Cap Plus Thinking Zap: tDCS of Frontopolar Cortex Improves Creative
744 Analogical Reasoning and Facilitates Conscious Augmentation of State Creativity in Verb
745 Generation. *Cereb. Cortex N. Y. NY.* **27**, 2628–2639 (2017).

746 25. T. Merten, I. Fischer, Creativity, personality and word association responses: associative
747 behaviour in forty supposedly creative persons. *Personal. Individ. Differ.* **27**, 933–942 (1999).

748 26. A. Gruszka, E. Nęcka, Priming and acceptance of close and remote associations by creative and
749 less creative people. *Creat. Res. J.* **14**, 193–205 (2002).

750 27. R. Prabhakaran, A. E. Green, J. R. Gray, Thin slices of creativity: Using single-word utterances
751 to assess creative cognition. *Behav. Res. Methods.* **46**, 641–659 (2014).

752 28. M. Benedek, J. Jurisch, K. Koschutnig, A. Fink, R. E. Beaty, Elements of creative thought:
753 Investigating the cognitive and neural correlates of association and bi-association processes.
754 *NeuroImage*. **210**, 116586 (2020).

755 29. C. S. Q. Siew, D. U. Wulff, N. M. Beckage, Y. N. Kenett, Cognitive Network Science: A Review
756 of Research on Cognition through the Lens of Network Representations, Processes, and
757 Dynamics. *Complexity*. **2019**, e2108423 (2019).

758 30. A. Baronchelli, R. Ferrer-i-Cancho, R. Pastor-Satorras, N. Chater, M. H. Christiansen, Networks
759 in cognitive science. *Trends Cogn. Sci.* **17**, 348–360 (2013).

760 31. J. Borge-Holthoefer, A. Arenas, Semantic Networks: Structure and Dynamics. *Entropy*. **12**,
761 1264–1302 (2010).

762 32. J. Borge-Holthoefer, A. Arenas, in *Int. j. complex syst. sci.* (2011;
763 <https://zaguan.unizar.es/record/61329>).

764 33. Y. N. Kenett, in *Exploring Transdisciplinarity in Art and Sciences*, Z. Kapoula, E. Volle, J.
765 Renoult, M. Andreatta, Eds. (Springer International Publishing, Cham, 2018;
766 https://doi.org/10.1007/978-3-319-76054-4_3), pp. 49–75.

767 34. Y. N. Kenett, M. Faust, A Semantic Network Cartography of the Creative Mind. *Trends Cogn. Sci.* **23**, 271–274 (2019).

769 35. A. L. Cosgrove, Y. N. Kenett, R. E. Beaty, M. T. Diaz, Quantifying flexibility in thought: The
770 resiliency of semantic networks differs across the lifespan. *Cognition*. **211**, 104631 (2021).

771 36. M. Benedek, Y. N. Kenett, K. Umdasch, D. Anaki, M. Faust, A. C. Neubauer, How semantic
772 memory structure and intelligence contribute to creative thought: a network science approach.
773 *Think. Reason.* **23**, 158–183 (2017).

774 37. M. Bernard, Y. Kenett, M. Ovando-Tellez, M. Benedek, E. Volle, *Building Individual Semantic
775 Networks and Exploring their Relationships with Creativity* (2019).

776 38. L. He, Y. N. Kenett, K. Zhuang, C. Liu, R. Zeng, T. Yan, T. Huo, J. Qiu, The relation between
777 semantic memory structure, associative abilities, and verbal and figural creativity. *Think. Reason.*
778 **27**, 268–293 (2021).

779 39. M. A. Runco, G. J. Jaeger, The Standard Definition of Creativity. *Creat. Res. J.* **24**, 92–96 (2012).

780 40. S. Acar, M. A. Runco, Divergent thinking: New methods, recent research, and extended theory.
781 *Psychol. Aesthet. Creat. Arts.* **13**, 153–158 (2019).

782 41. T. Yan, K. Zhuang, L. He, C. Liu, R. Zeng, J. Qiu, Left temporal pole contributes to creative
783 thinking via an individual semantic network. *Psychophysiology*. e13841 (2021).

784 42. J. Diedrich, E. Jauk, P. J. Silvia, J. M. Gredlein, A. C. Neubauer, M. Benedek, Assessment of
785 real-life creativity: The Inventory of Creative Activities and Achievements (ICAA). *Psychol.
786 Aesthet. Creat. Arts.* **12**, 304–316 (2018).

787 43. R. E. Beaty, Y. N. Kenett, A. P. Christensen, M. D. Rosenberg, M. Benedek, Q. Chen, A. Fink,
788 J. Qiu, T. R. Kwapil, M. J. Kane, P. J. Silvia, Robust prediction of individual creative ability
789 from brain functional connectivity. *Proc. Natl. Acad. Sci.* **115**, 1087–1092 (2018).

790 44. G. Gonen-Yaacovi, L. C. de Souza, R. Levy, M. Urbanski, G. Josse, E. Volle, Rostral and caudal
791 prefrontal contribution to creativity: a meta-analysis of functional imaging data. *Front. Hum.
792 Neurosci.* **7** (2013), doi:10.3389/fnhum.2013.00465.

793 45. M. Boccia, L. Piccardi, L. Palermo, R. Nori, M. Palmiero, Where do bright ideas occur in our
794 brain? Meta-analytic evidence from neuroimaging studies of domain-specific creativity. *Front.
795 Psychol.* **6** (2015), doi:10.3389/fpsyg.2015.01195.

796 46. M. Benedek, in *Exploring Transdisciplinarity in Art and Sciences*, Z. Kapoula, E. Volle, J.
797 Renoult, M. Andreatta, Eds. (Springer International Publishing, Cham, 2018;
798 https://doi.org/10.1007/978-3-319-76054-4_2), pp. 31–48.

799 47. R. E. Beaty, P. Seli, D. L. Schacter, Network Neuroscience of Creative Cognition: Mapping
800 Cognitive Mechanisms and Individual Differences in the Creative Brain. *Curr. Opin. Behav. Sci.*
801 **27**, 22–30 (2019).

802 48. D. L. Zabelina, J. R. Andrews-Hanna, Dynamic network interactions supporting internally-
803 oriented cognition. *Curr. Opin. Neurobiol.* **40**, 86–93 (2016).

804 49. C. Liu, Z. Ren, K. Zhuang, L. He, T. Yan, R. Zeng, J. Qiu, Semantic association ability mediates
805 the relationship between brain structure and human creativity. *Neuropsychologia*. **151**, 107722
806 (2021).

807 50. L. S. Cogdell-Brooke, P. T. Sowden, I. R. Violante, H. E. Thompson, A meta-analysis of
808 functional magnetic resonance imaging studies of divergent thinking using activation likelihood
809 estimation. *Hum. Brain Mapp.* **41**, 5057–5077 (2020).

810 51. M. Benedek, T. Schües, R. E. Beaty, E. Jauk, K. Koschutnig, A. Fink, A. C. Neubauer, To create
811 or to recall original ideas: Brain processes associated with the imagination of novel object uses.
812 *Cortex*. **99**, 93–102 (2018).

813 52. K. Madore, P. Thakral, R. Beaty, D. Addis, D. Schacter, Neural Mechanisms of Episodic
814 Retrieval Support Divergent Creative Thinking. *Cereb. Cortex N. Y. N* **29**, 1–17 (2017).

815 53. H. E. Matheson, Y. N. Kenett, The role of the motor system in generating creative thoughts.
816 *NeuroImage*. **213**, 116697 (2020).

817 54. T. Wei, X. Liang, Y. He, Y. Zang, Z. Han, A. Caramazza, Y. Bi, Predicting Conceptual
818 Processing Capacity from Spontaneous Neuronal Activity of the Left Middle Temporal Gyrus.
819 *J. Neurosci.* **32**, 481–489 (2012).

820 55. Q. Chen, W. Yang, W. Li, D. Wei, H. Li, Q. Lei, Q. Zhang, J. Qiu, Association of creative
821 achievement with cognitive flexibility by a combined voxel-based morphometry and resting-state
822 functional connectivity study. *NeuroImage*. **102 Pt 2**, 474–483 (2014).

823 56. X. Shen, E. S. Finn, D. Scheinost, M. D. Rosenberg, M. M. Chun, X. Papademetris, R. T.
824 Constable, Using connectome-based predictive modeling to predict individual behavior from
825 brain connectivity. *Nat. Protoc.* **12**, 506–518 (2017).

826 57. M. D. Rosenberg, E. S. Finn, D. Scheinost, X. Papademetris, X. Shen, R. T. Constable, M. M.
827 Chun, A neuromarker of sustained attention from whole-brain functional connectivity. *Nat.
828 Neurosci.* **19**, 165–171 (2016).

829 58. E. Frith, D. B. Elbich, A. P. Christensen, M. D. Rosenberg, Q. Chen, M. J. Kane, P. J. Silvia, P.
830 Seli, R. E. Beaty, Intelligence and creativity share a common cognitive and neural basis. *J. Exp.
831 Psychol. Gen.* **150**, 609–632 (2021).

832 59. E. V. Goldfarb, M. D. Rosenberg, D. Seo, R. T. Constable, R. Sinha, Hippocampal seed
833 connectome-based modeling predicts the feeling of stress. *Nat. Commun.* **11**, 2650 (2020).

834 60. Z. Ren, R. J. Daker, L. Shi, J. Sun, R. E. Beaty, X. Wu, Q. Chen, W. Yang, I. M. Lyons, A. E.
835 Green, J. Qiu, Connectome-Based Predictive Modeling of Creativity Anxiety. *NeuroImage*. **225**,
836 117469 (2021).

837 61. P. Liu, W. Yang, K. Zhuang, D. Wei, R. Yu, X. Huang, J. Qiu, The functional connectome
838 predicts feeling of stress on regular days and during the COVID-19 pandemic. *Neurobiol. Stress.*
839 **14**, 100285 (2021).

840 62. M. D. Humphries, K. Gurney, Network ‘Small-World-Ness’: A Quantitative Method for
841 Determining Canonical Network Equivalence. *PLOS ONE*. **3**, e0002051 (2008).

842 63. A. Schaefer, R. Kong, E. M. Gordon, T. O. Laumann, X.-N. Zuo, A. J. Holmes, S. B. Eickhoff,
843 B. T. T. Yeo, Local-Global Parcellation of the Human Cerebral Cortex from Intrinsic Functional
844 Connectivity MRI. *Cereb. Cortex N. Y. N* **28**, 3095–3114 (2018).

845 64. D. J. Watts, S. H. Strogatz, Collective dynamics of ‘small-world’ networks. *Nature*. **393**, 440–
846 442 (1998).

847 65. O. Sporns, The human connectome: a complex network. *Ann. N. Y. Acad. Sci.* **1224**, 109–125
848 (2011).

849 66. F. De Vico Fallani, J. Richiardi, M. Chavez, S. Achard, Graph analysis of functional brain
850 networks: practical issues in translational neuroscience. *Philos. Trans. R. Soc. B Biol. Sci.* **369**,
851 20130521 (2014).

852 67. Y. N. Kenett, R. Gold, M. Faust, The hyper-modular associative mind: A computational analysis
853 of associative responses of persons with Asperger syndrome. *Lang. Speech.* **59**, 297–317 (2016).

854 68. C. S. Q. Siew, Community structure in the phonological network. *Front. Psychol.* **4** (2013),
855 doi:10.3389/fpsyg.2013.00553.

856 69. R. E. Beaty, M. Benedek, S. Barry Kaufman, P. J. Silvia, Default and Executive Network
857 Coupling Supports Creative Idea Production. *Sci. Rep.* **5**, 10964 (2015).

858 70. L. Aziz-Zadeh, S.-L. Liew, F. Dandekar, Exploring the neural correlates of visual creativity. *Soc.*
859 *Cogn. Affect. Neurosci.* **8**, 475–480 (2013).

860 71. Q. Chen, R. E. Beaty, Z. Cui, J. Sun, H. He, K. Zhuang, Z. Ren, G. Liu, J. Qiu, Brain hemispheric
861 involvement in visuospatial and verbal divergent thinking. *NeuroImage*. **202**, 116065 (2019).

862 72. M. E. Raichle, The restless brain: how intrinsic activity organizes brain function. *Philos. Trans. R. Soc. Lond. B. Biol. Sci.* **370** (2015), doi:10.1098/rstb.2014.0172.

864 73. T. R. Marron, Y. Lerner, E. Berant, S. Kinreich, I. Shapira-Lichter, T. Hendler, M. Faust, Chain
865 free association, creativity, and the default mode network. *Neuropsychologia*. **118**, 40–58 (2018).

866 74. R. E. Beaty, A. P. Christensen, M. Benedek, P. J. Silvia, D. L. Schacter, Creative constraints:
867 Brain activity and network dynamics underlying semantic interference during idea production.
868 *NeuroImage*. **148**, 189–196 (2017).

869 75. E. Mandonnet, M. Vincent, A. Valero-Cabré, V. Facque, M. Barberis, F. Bonnetblanc, F.
870 Rheault, E. Volle, M. Descoteaux, D. S. Margulies, Network-level causal analysis of set-shifting
871 during trail making test part B: A multimodal analysis of a glioma surgery case. *Cortex J. Devoted Study Nerv. Syst. Behav.* **132**, 238–249 (2020).

873 76. A. L. Pinho, F. Ullén, M. Castelo-Branco, P. Fransson, Ö. de Manzano, Addressing a Paradox:
874 Dual Strategies for Creative Performance in Introspective and Extrospective Networks. *Cereb. Cortex*. **26**, 3052–3063 (2016).

876 77. S. Liu, M. G. Erkkinen, M. L. Healey, Y. Xu, K. E. Swett, H. M. Chow, A. R. Braun, Brain
877 activity and connectivity during poetry composition: Toward a multidimensional model of the
878 creative process. *Hum. Brain Mapp.* **36**, 3351–3372 (2015).

879 78. M. Ellamil, C. Dobson, M. Beeman, K. Christoff, Evaluative and generative modes of thought
880 during the creative process. *NeuroImage*. **59**, 1783–1794 (2012).

881 79. L. Q. Uddin, Salience processing and insular cortical function and dysfunction. *Nat. Rev. Neurosci.* **16**, 55–61 (2015).

883 80. A. L. Pinho, O. de Manzano, P. Fransson, H. Eriksson, F. Ullen, Connecting to Create: Expertise
884 in Musical Improvisation Is Associated with Increased Functional Connectivity between
885 Premotor and Prefrontal Areas. *J. Neurosci.* **34**, 6156–6163 (2014).

886 81. R. E. Beaty, The neuroscience of musical improvisation. *Neurosci. Biobehav. Rev.* **51**, 108–117
887 (2015).

888 82. Q. Chen, R. E. Beaty, J. Qiu, Mapping the artistic brain: Common and distinct neural activations
889 associated with musical, drawing, and literary creativity. *Hum. Brain Mapp.* **41**, 3403–3419
890 (2020).

891 83. C. J. Limb, A. R. Braun, Neural Substrates of Spontaneous Musical Performance: An fMRI Study
892 of Jazz Improvisation. *PLoS ONE.* **3**, e1679 (2008).

893 84. K. Japardi, S. Bookheimer, K. Knudsen, D. G. Ghahremani, R. M. Bilder, Functional magnetic
894 resonance imaging of divergent and convergent thinking in Big-C creativity. *Neuropsychologia.*
895 **118**, 59–67 (2018).

896 85. J. R. Binder, R. H. Desai, The neurobiology of semantic memory. *Trends Cogn. Sci.* **15**, 527–
897 536 (2011).

898 86. R. E. Jung, The structure of creative cognition in the human brain. *Front. Hum. Neurosci.* **7**
899 (2013), doi:10.3389/fnhum.2013.00330.

900 87. M. Benedek, in *The Cambridge Handbook of the Neuroscience of Creativity*, R. E. Jung, O.
901 Vartanian, Eds. (Cambridge University Press, ed. 1, 2018;
902 https://www.cambridge.org/core/product/identifier/9781316556238%23CN-bp-10/type/book_part), pp. 180–194.

904 88. T. Asari, S. Konishi, K. Jimura, J. Chikazoe, N. Nakamura, Y. Miyashita, Right temporopolar
905 activation associated with unique perception. *NeuroImage.* **41**, 145–152 (2008).

906 89. L. Aziz-Zadeh, J. T. Kaplan, M. Iacoboni, “Aha!”: The neural correlates of verbal insight
907 solutions. *Hum. Brain Mapp.* **30**, 908–916 (2009).

908 90. A. Abraham, S. Beudt, D. V. M. Ott, D. Yves von Cramon, Creative cognition and the brain:
909 Dissociations between frontal, parietal–temporal and basal ganglia groups. *Brain Res.* **1482**, 55–
910 70 (2012).

911 91. M. A. Lambon Ralph, Neurocognitive insights on conceptual knowledge and its breakdown.
912 *Philos. Trans. R. Soc. B Biol. Sci.* **369**, 20120392 (2014).

913 92. M. A. Lambon Ralph, S. Ehsan, G. A. Baker, T. T. Rogers, Semantic memory is impaired in
914 patients with unilateral anterior temporal lobe resection for temporal lobe epilepsy. *Brain.* **135**,
915 242–258 (2012).

916 93. B. Garcin, M. Urbanski, M. Thiebaut de Schotten, R. Levy, E. Volle, Anterior Temporal Lobe
917 Morphometry Predicts Categorization Ability. *Front. Hum. Neurosci.* **12** (2018),
918 doi:10.3389/fnhum.2018.00036.

919 94. C. Aichelburg, M. Urbanski, M. Thiebaut de Schotten, F. Humbert, R. Levy, E. Volle,
920 Morphometry of Left Frontal and Temporal Poles Predicts Analogical Reasoning Abilities.
921 *Cereb. Cortex.* **26**, 915–932 (2016).

922 95. B. Shi, X. Cao, Q. Chen, K. Zhuang, J. Qiu, Different brain structures associated with artistic and
923 scientific creativity: a voxel-based morphometry study. *Sci. Rep.* **7**, 42911 (2017).

924 96. A. Abraham, K. Pieritz, K. Thybusch, B. Rutter, S. Kröger, J. Schreckendiek, R. Stark, S.
925 Windmann, C. Hermann, Creativity and the brain: Uncovering the neural signature of conceptual
926 expansion. *Neuropsychologia*. **50**, 1906–1917 (2012).

927 97. A. Abraham, B. Rutter, T. Bantin, C. Hermann, Creative conceptual expansion: A combined
928 fMRI replication and extension study to examine individual differences in creativity.
929 *Neuropsychologia*. **118**, 29–39 (2018).

930 98. M. Benedek, E. Jauk, A. Fink, K. Koschutnig, G. Reishofer, F. Ebner, A. C. Neubauer, To create
931 or to recall? Neural mechanisms underlying the generation of creative new ideas. *NeuroImage*.
932 **88**, 125–133 (2014).

933 99. E. G. Chrysikou, H. M. Morrow, A. Flohrschutz, L. Denney, Augmenting ideational fluency in
934 a creativity task across multiple transcranial direct current stimulation montages. *Sci. Rep.* **11**,
935 8874 (2021).

936 100. M. Jung-Beeman, Bilateral brain processes for comprehending natural language. *Trends Cogn. Sci.* **9**, 512–518 (2005).

938 101. C. Chiarello, N. A. Kacinik, C. Shears, S. R. Arambel, L. K. Halderman, C. S. Robinson,
939 Exploring cerebral asymmetries for the verb generation task. *Neuropsychology*. **20**, 88–104
940 (2006).

941 102. K. C. Aberg, K. C. Doell, S. Schwartz, The “Creative Right Brain” Revisited: Individual
942 Creativity and Associative Priming in the Right Hemisphere Relate to Hemispheric Asymmetries
943 in Reward Brain Function. *Cereb. Cortex*. **27**, 4946–4959 (2017).

944 103. T. Lubart, F. Zenasni, B. Barbot, Creative potential and its measurement. *Int. J. Talent Dev. Creat.* **1**, 41–50 (2013).

946 104. J. A. Plucker, M. Karwowski, J. C. Kaufman, in *The Cambridge handbook of intelligence*, 2nd ed (Cambridge University Press, New York, NY, US, 2020), pp. 1087–1105.

948 105. G. J. Feist, A Meta-Analysis of Personality in Scientific and Artistic Creativity. *Personal. Soc. Psychol. Rev.* **2**, 290–309 (1998).

950 106. M. Karwowski, M. Czerwonka, E. Wiśniewska, B. Forthmann, How Is Intelligence Test
951 Performance Associated with Creative Achievement? A Meta-Analysis. *J. Intell.* **9**, 28 (2021).

952 107. M. Debrenne, *Le dictionnaire des associations verbales du français et ses applications* (2011).

953 108. Y. N. Kenett, E. Levi, D. Anaki, M. Faust, The semantic distance task: Quantifying semantic
954 distance with semantic network path length. *J. Exp. Psychol. Learn. Mem. Cogn.* **43**, 1470–1489
955 (2017).

956 109. A. A. Kumar, D. A. Balota, M. Steyvers, Distant connectivity and multiple-step priming in large-
957 scale semantic networks. *J. Exp. Psychol. Learn. Mem. Cogn.* **46**, 2261–2276 (2020).

958 110. M. E. J. Newman, Modularity and community structure in networks. *Proc. Natl. Acad. Sci.* **103**,
959 8577–8582 (2006).

960 111. S. Fortunato, Community detection in graphs. *Phys. Rep.* **486**, 75–174 (2010).

961 112. M. Rubinov, O. Sporns, Weight-conserving characterization of complex functional brain
962 networks. *NeuroImage*. **56**, 2068–2079 (2011).

963 113. E. Jauk, M. Benedek, A. C. Neubauer, The Road to Creative Achievement: A Latent Variable
964 Model of Ability and Personality Predictors. *Eur. J. Personal.* **28**, 95–105 (2014).

965 114. R. W. Cox, AFNI: software for analysis and visualization of functional magnetic resonance
966 neuroimages. *Comput. Biomed. Res. Int. J.* **29**, 162–173 (1996).

967 115. P. Kundu, N. D. Brenowitz, V. Voon, Y. Worbe, P. E. Vértes, S. J. Inati, Z. S. Saad, P. A.
968 Bandettini, E. T. Bullmore, Integrated strategy for improving functional connectivity mapping
969 using multiecho fMRI. *Proc. Natl. Acad. Sci.* **110**, 16187–16192 (2013).

970 116. P. Kundu, S. J. Inati, J. W. Evans, W.-M. Luh, P. A. Bandettini, Differentiating BOLD and non-
971 BOLD signals in fMRI time series using multi-echo EPI. *NeuroImage*. **60**, 1759–1770 (2012).

972 117. The tedana Community, Z. Ahmed, P. A. Bandettini, K. L. Bottenhorn, C. Caballero-Gaudes, L.
973 T. Dowdle, E. DuPre, J. Gonzalez-Castillo, D. Handwerker, S. Heunis, P. Kundu, A. R. Laird,
974 R. Markello, C. J. Markiewicz, T. Maullin-Sapey, S. Moia, T. Salo, I. Staden, J. Teves, E.
975 Uruñuela, M. Vaziri-Pashkam, K. Whitaker, *ME-ICA/tedana: 0.0.10* (Zenodo, 2021;
976 https://zenodo.org/record/4725985#.YKjmQus6_RU).

977 118. C. J. Lynch, J. D. Power, M. A. Scult, M. Dubin, F. M. Gunning, C. Liston, Rapid Precision
978 Functional Mapping of Individuals Using Multi-Echo fMRI. *Cell Rep.* **33**, 108540 (2020).

979 119. C. Gaser, R. Dahnke, CAT-A Computational Anatomy Toolbox for the Analysis of Structural
980 MRI Data (2016), (available at [/paper/CAT-A-Computational-Anatomy-Toolbox-for-the-of-MRI-Gaser-Dahnke/2682c2c5f925da18f465952f1a5c904202ab2693](https://paper/CAT-A-Computational-Anatomy-Toolbox-for-the-of-MRI-Gaser-Dahnke/2682c2c5f925da18f465952f1a5c904202ab2693)).

982 120. A. Abraham, F. Pedregosa, M. Eickenberg, P. Gervais, A. Mueller, J. Kossaifi, A. Gramfort, B.
983 Thirion, G. Varoquaux, Machine learning for neuroimaging with scikit-learn. *Front. Neuroinformatics*. **8** (2014), doi:10.3389/fninf.2014.00014.

985 121. G. van Rossum, Python reference manual (1995) (available at <https://ir.cwi.nl/pub/5008>).

986 122. J. D. Power, A. Mitra, T. O. Laumann, A. Z. Snyder, B. L. Schlaggar, S. E. Petersen, Methods to
987 detect, characterize, and remove motion artifact in resting state fMRI. *NeuroImage*. **84** (2014),
988 doi:10.1016/j.neuroimage.2013.08.048.

989 123. A. Fornito, A. Zalesky, M. Breakspear, Graph analysis of the human connectome: promise,
990 progress, and pitfalls. *NeuroImage*. **80**, 426–444 (2013).

991 124. V. Latora, M. Marchiori, Efficient behavior of small-world networks. *Phys. Rev. Lett.* **87**, 198701
992 (2001).

993 125. O. Sporns, C. J. Honey, Small worlds inside big brains. *Proc. Natl. Acad. Sci.* **103**, 19219–19220
994 (2006).

995 126. E. Bullmore, O. Sporns, Complex brain networks: graph theoretical analysis of structural and
996 functional systems. *Nat. Rev. Neurosci.* **10**, 186–198 (2009).

997 127. D. S. Bassett, E. Bullmore, Small-World Brain Networks. *The Neuroscientist*. **12**, 512–523
998 (2006).

999 128. M. Xia, J. Wang, Y. He, BrainNet Viewer: A Network Visualization Tool for Human Brain
1000 Connectomics. *PLoS ONE*. **8**, e68910 (2013).

1001 129. K. J. Preacher, A. F. Hayes, SPSS and SAS procedures for estimating indirect effects in simple
1002 mediation models. *Behav. Res. Methods Instrum. Comput.* **36**, 717–731 (2004).

1003 130. A. F. Hayes, Beyond Baron and Kenny: Statistical Mediation Analysis in the New Millennium.
1004 *Commun. Monogr.* **76**, 408–420 (2009).

1005 131. D. D. Rucker, K. J. Preacher, Z. L. Tormala, R. E. Petty, Mediation Analysis in Social
1006 Psychology: Current Practices and New Recommendations: Mediation Analysis in Social
1007 Psychology. *Soc. Personal. Psychol. Compass.* **5**, 359–371 (2011).

1008 132. A. F. Hayes, A. K. Montoya, A Tutorial on Testing, Visualizing, and Probing an Interaction
1009 Involving a Multicategorical Variable in Linear Regression Analysis. *Commun. Methods Meas.*
1010 **11**, 1–30 (2017).

1011

1012 Acknowledgments

1013 We thank D. Margulies, A. Lopez-Persem, F. De Vico Fallani, M. Chavez for advice and helpful
1014 discussion and commentary. We also thank the participants for making this work possible.

1015

1016 Funding

1017

1018 The research was supported by "Agence Nationale de la Recherche" [grant numbers ANR-19-CE37-
1019 0001-01] (EV) and received infrastructure funding from the French programs "Investissements d'avenir"
1020 ANR-11-INBS-0006 (EV) and ANR-10-IAIHU-06 (EV). This work was also funded by Becas-Chile of
1021 ANID-CONICYT (MOT). The funder had no role in study design, data collection and analysis, decision
1022 to publish, or preparation of the manuscript.

1023

1024 Author Contributions

1025 EV, YNK and MBEN designed the study. MOT, MBER and JB collected the data. MOT analyzed the
1026 data with contribution from BB, MBER, TB, JB, EV, and YNK. MOT wrote the first draft of the article.
1027 MOT, YNK, MBEN, BB and EV wrote and revised the manuscript. All authors revised and approved
1028 the manuscript.

1029

1030 Competing Interests

1031 The authors declare no competing interests.

1032 Data and materials availability

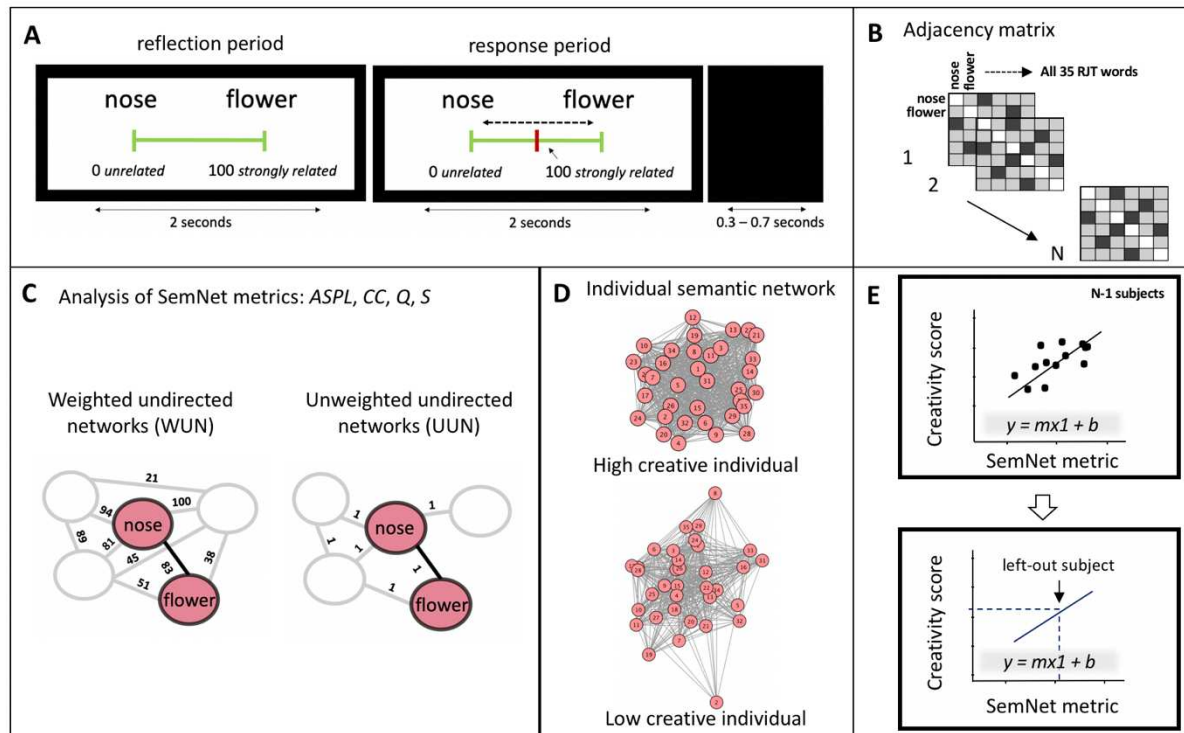
1033

1034 The data that support the findings of this study can be available on request from the corresponding
1035 author. All the data used in this study were collected on the PRISME and CENIR platforms at the Paris
1036 Brain Institute (ICM). Most analyses were conducted using open softwares and toolboxes available
1037 online (SPM, AFNI, Nilearn and TEDANA) and using homemade scripts. Custom codes are available
1038 from the corresponding authors on request.

1039

1040

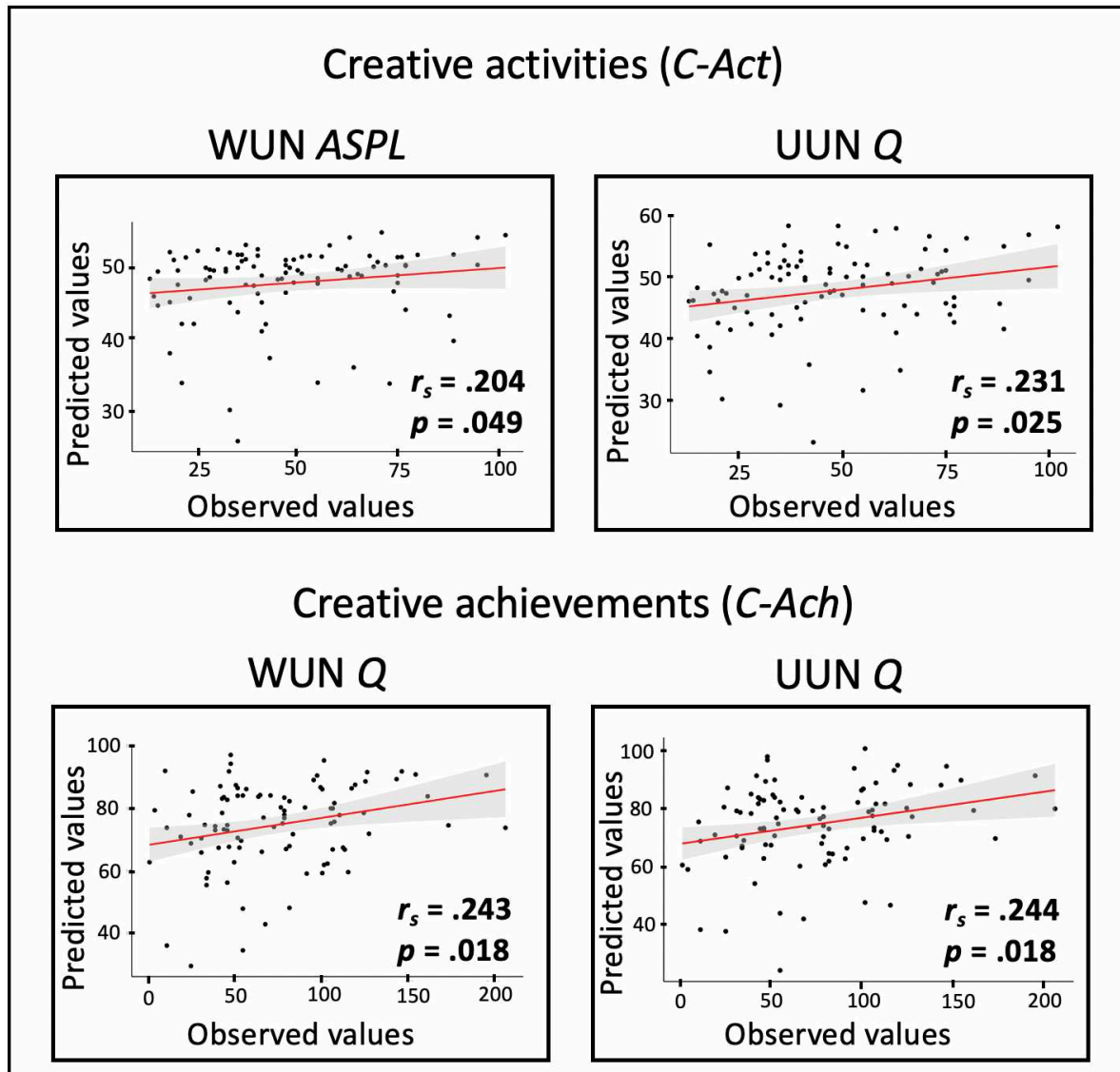
1041 **Figures**



1042

1043 **Figure 1. Estimation of individual semantic networks (SemNets) to predict creativity.** (A) Trial
1044 representation of an exemplary trial of the RJT asking participants to judge the relatedness of 595 word
1045 pairs. Each trial began with the display of a pair of words along with a visual scale (reflection period)
1046 ranging from 0 (unrelated words) to 100 (strongly related words). During the next 2 seconds (response
1047 period), participants were allowed to move the cursor (in red) using a trackball to indicate the relatedness
1048 of the two words. An intertrial interval of 0.3-0.7s separated trials. (B) For each participant, we
1049 computed a 35 by 35 adjacency (connectivity) matrix with columns and rows representing each of the
1050 35 RJT words, and cell values correspond to the relatedness judgments given by the participant during
1051 the RJT. (C) We estimated individual semantic memory networks following two established approaches:
1052 weighted (WUN) and unweighted (UUN) undirected networks, using the RJT words as the network
1053 nodes. In the WUN networks, the RJT judgments reflected the strength of links between nodes. In the
1054 UUN networks, the RJT judgments above average (50) were kept and set to one. The SemNet metrics
1055 were computed for both WUN and UUN separately: ASPL, CC, Q and S. (D) Representation of the
1056 individual WUN SemNets for a low creative and a high creative participant. (E) Linear regressions using
1057 leave-one-out cross-validations were performed to explore whether real-life creative activities (C-Act)
1058 and achievements (C-Ach) were predicted from SemNet properties estimated in (b). The SemNet metrics
1059 were used to build predictive linear models in N-1 participants. The predictive model was tested on the
1060 left-out participant using its SemNet metric (m) to predict its creativity scores. RJT = relatedness
1061 judgment task; SemNet = semantic network; ASPL = average shortest path length; CC = clustering
1062 coefficient; Q = modularity; S = small-worldness.

1063



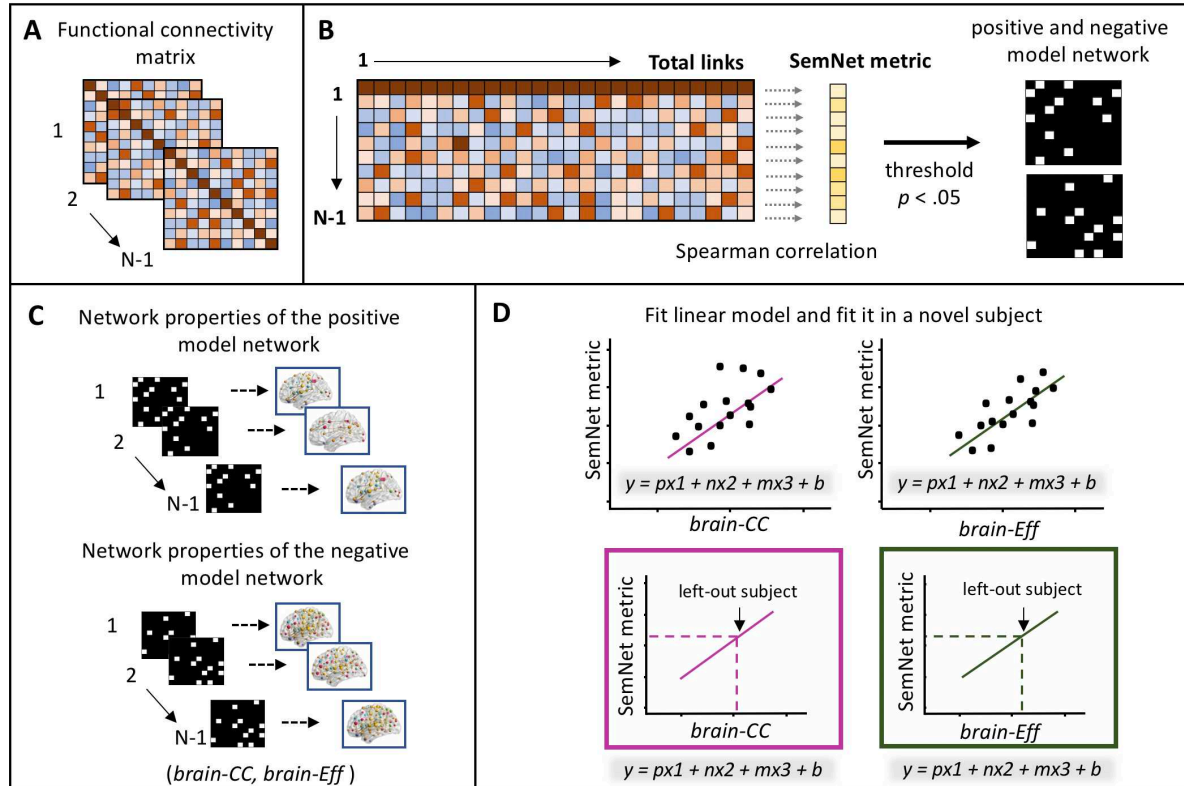
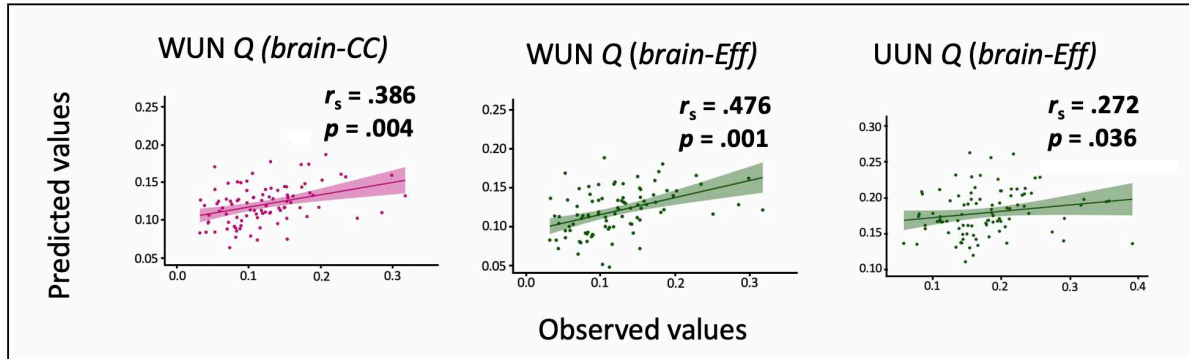


Figure 3. Connectome Predictive Modeling-based prediction method. (A) We defined the brain nodes based on the Schaefer atlas consisting of 200 ROIs (63). For each participant, we assessed the BOLD activity during the RJT in each ROI and used pairwise Pearson correlations to estimate a 200 by 200 task-related functional connectivity matrix. Using a leave-one-out approach, all of the CPM steps were conducted in $N-1$ participants. (B) The functional connectivity matrix (all links) was correlated to SemNet metrics using Spearman correlations. The links that significantly positively or negatively correlated with the SemNet metric ($p < .05$) formed a positive and a negative model network, respectively. (C) We calculated two network properties (in separate CPM analyses) of the positive and negative model networks, *brain-CC* and *brain-Eff* metrics. (D) The brain metrics in the positive (p) and negative (n) model networks were used to build a linear model predicting the SemNet metric in the left-out participant. Since head motion can impact CPM, we included the meanFD variable (m), a head motion parameter, as a regressor in the model to avoid a possible effect in the prediction. Finally, the model was applied to the left-out participant to compute a predicted SemNet value from his/her brain model networks. The predicted value was then correlated with the observed value to assess the model predictive validity.



1090
1091

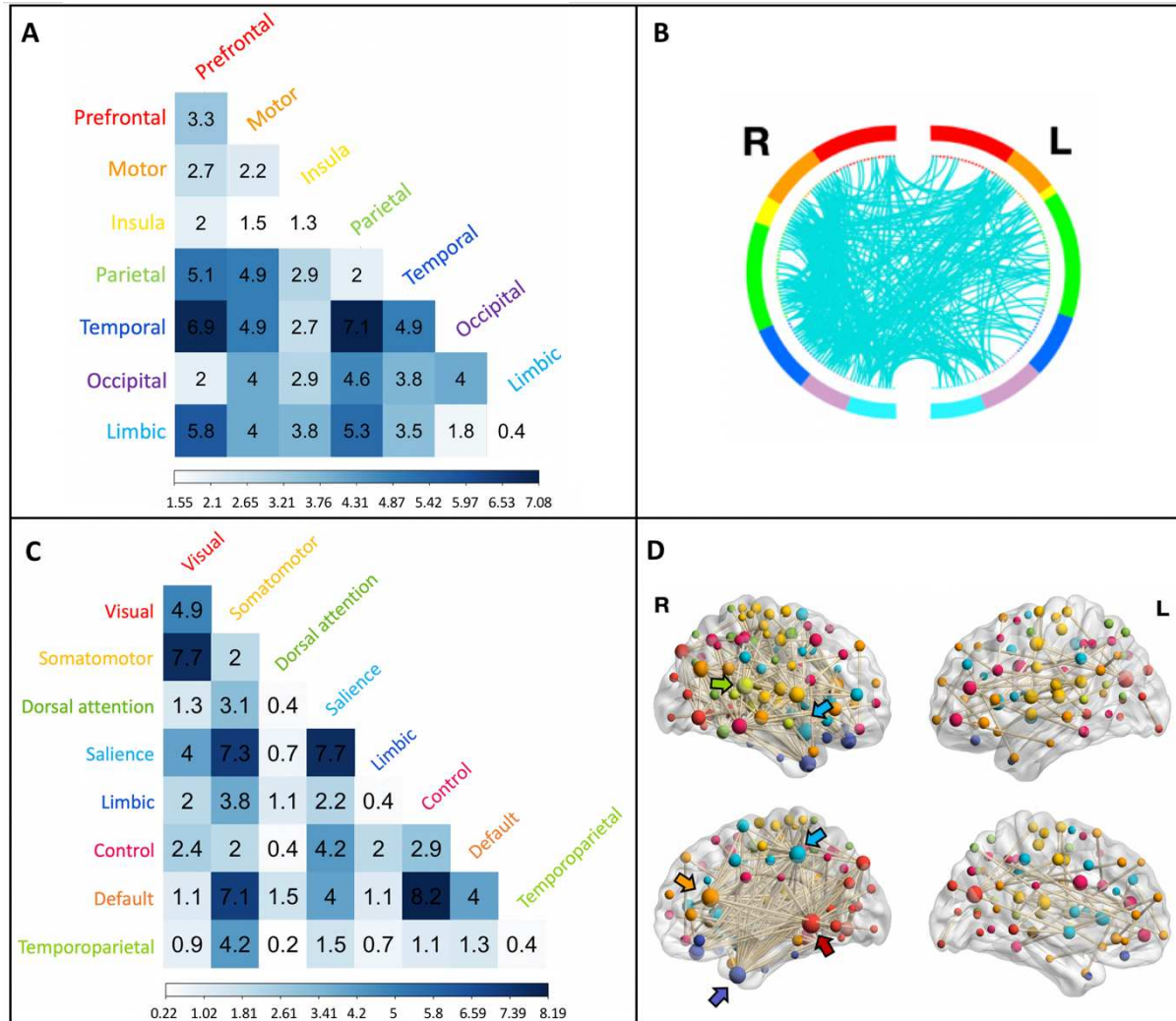
1092 **Figure 4. Predicted and observed SemNet metrics.** The plots show the Spearman correlations between
1093 the predicted values (y-axis) and observed values (x-axis) of SemNet metrics based on brain connectivity
1094 for the significant predictions. Green plots are presented for *brain-Eff* and magenta ones for *brain-CC*.
1095 In the upper-right side of each plot, we present the r_s and the p values. The reported p values are based
1096 on permutation testing.

1097

1098

1099

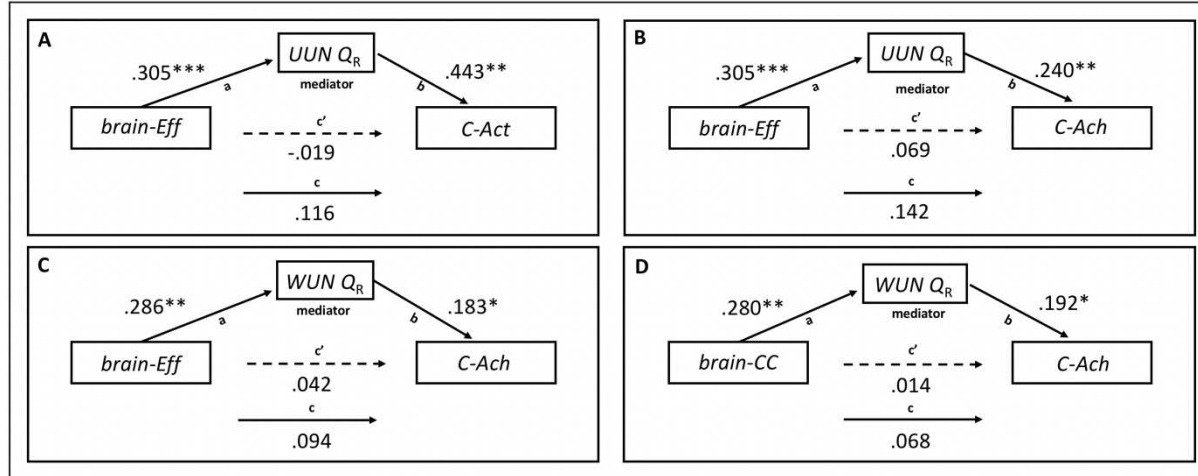
1100



1101
1102

1103 **Figure 5. Functional anatomy of the CPM model predicting the SemNet metric UUN Q .** (A) First,
1104 we examined the distribution of the links of the model network at the brain location level, specifically
1105 into the brain lobes. The correlation matrix represents the percentage of links within the model network
1106 connecting seven different brain lobes (total links = 452). (B) A circular graph represents the distribution
1107 of links within and between brain regions in the left and right hemispheres. Brain regions are color-
1108 coded as in (A), and the cyan lines represent the links connecting the ROIs. For visualization purposes,
1109 we used a nodal degree threshold of $k > 10$. (C) Second, we examined the distribution of the links across
1110 intrinsic functional networks based on Schaefer's atlas (63). The matrix represents the percentage of
1111 links within the model network occurring within and between eight intrinsic brain networks. (D) The
1112 nodes and links of the model network are superimposed on a volume rendering of the brain. The color
1113 of the nodes represents the functional network they belong to, using a similar color code as in (B). The
1114 size of the nodes is proportional to their degree, and the highest degree nodes are marked by arrows.
1115 Nodes with degree $k = 0$ are not displayed.

1116



1117
1118
1119 **Figure 6. Mediation Analyses.** Results of the mediation models are presented in path diagrams. Each
1120 indicates the beta weights of the regression coefficients with the brain metrics of the model
1121 network (*brain-Eff* and *brain-CC*) as the independent variable (predictor), SemNet metrics as the
1122 mediator (*UUN Q_R* and *WUN Q_R*), and real-life creativity (*C-Act* and *C-Ach*) as the dependent variable
1123 (outcome). The total effect is indicated by path *c*, the direct effect by path *c'*, and the indirect effect is
1124 given by the product of path *a* and path *b*. The indirect effect was significant in all the reported
1125 mediations (A) The mediating role of *UUN Q* on the relationship between the *brain-Eff* of the brain
1126 functional network predicting it and *C-Act*. (B) Mediating role of *UUN Q* between the *brain-Eff* of the
1127 brain network predicting it and *C-Ach*. (C) Mediating role of the weighted networks *WUN Q* on the
1128 relationship between the *brain-Eff* of the functional connectivity of the negative model network
1129 predicting it and *C-Ach*. (D) Mediating role of *WUN Q* on the relationship between the *brain-CC* of the
1130 functional connectivity of the negative model network predicting it and *C-Ach*. * $p < .05$; ** $p < .01$;
1131 *** $p < .001$

1132

1133

1134

1135

1136

1137

1138

1139

1140

1141 **Tables**

1142
1143 **Table 1. Descriptive statistics of creativity scores and semantic network measures.** Data are shown
1144 for real-life creativity activities (*C-Act*) and achievements (*C-Ach*), and for SemNet metrics of weighted
1145 (WUN) and unweighted (UUN) networks.
1146
1147

	<i>Mean</i>	<i>SD</i>	<i>Min</i>	<i>Max</i>
Creativity scores				
<i>C-Act</i>	47.894	21.695	13	102
<i>C-Ach</i>	74.638	42.249	1	207
WUN metrics				
<i>ASPL</i>	0.021	0.004	0.015	0.037
<i>CC</i>	0.363	0.096	0.142	0.628
<i>Q</i>	0.122	0.058	0.032	0.319
<i>S</i>	1.003	0.073	0.828	1.387
UUN metrics				
<i>ASPL</i>	1.633	0.221	1.262	2.361
<i>CC</i>	0.585	0.082	0.438	0.781
<i>Q</i>	0.178	0.064	0.058	0.392
<i>S</i>	1.386	0.271	1.011	2.936

1148
1149 Note. *ASPL*= Average Shortest Path Length; *CC* = Clustering coefficient; *Q* = Modularity; *S* = Small-
1150 Worldness.
1151
1152

1153 **Table 2. Relationship between individual semantic network metrics and creativity.** The Spearman
1154 correlations between SemNet metrics and creativity scores are reported (r_s for *C-Act* and *C-Ach*). In bold
1155 are the significant predictions of creativity from the SemNet properties after permutation testing shown
1156 in **Figure 2**. * indicate correlations that reached significance after FDR correction for multiple
1157 comparisons.
1158

	Creativity scores		<i>C-Act</i>		<i>C-Ach</i>	
	r_s	<i>p</i>	r_s	<i>p</i>	r_s	<i>p</i>
WUN metrics						
<i>ASPL</i>	-.276	.007*	-.208	.044		
<i>CC</i>	.165	.111	.201	.052		
<i>Q</i>	-.179	.085	-.295	.004*		
<i>S</i>	.234	.023	-.017	.868		
UUN metrics						
<i>ASPL</i>	-.125	.230	-.149	.152		
<i>CC</i>	.092	.378	.080	.441		
<i>Q</i>	-.281	.006*	-.287	.005*		
<i>S</i>	-.154	.139	-.219	.034		

1159
1160